1. Introduction

Heart failure (HF) is one of the leading causes of premature death and poor quality of life. Community-based epidemiological studies have provided much-needed information on the demography of HF, requiring insight into its influence on public health. In most patients, chronic HF is accompanied by a range of concomitant disorders that contribute to the cause of the disease and play a key role in its progression and response to treatment (Krum & Gilbert, 2003).

Although several pharmacological agents have improved both the mortality and morbidity of patients with advanced HF (for review, see Jessup & Brozena, 2003), no treatment is available to completely prevent its progression except cardiac transplantation. However, the transplantation encompasses a variety of socioeconomic problems in addition to its medical limitations. End-stage dilated cardiomyopathy (DCM) is the condition that most frequently requires heart transplantation in Japan. The hereditary origin of DCM is estimated to account for ~20% to 30% of all patients with DCM (Michels et al., 1992; Towbin & Bowles, 2002).

2. Dystrophin and dystrophin-associated proteins

Dystrophin (Dys) and Dys-associated proteins (DAP) are located in sarcolemma (SL) of cardiac and skeletal muscles and in plasma membrane of central nervous system or retina (Cox & Kunkel, 1997; Henry & Campbell, 1999). Dys is a rod-like protein that lies beneath the SL and forms part of a system which links actin on the inside of muscle fibers, through DAP to extracellular matrix proteins, laminin α2 (Fig. 1). DAP contain 2 groups of membrane proteins: dystroglycans (DGs) and sarcoglycans (SGs, Cox & Kunkel, 1997; Holt et al., 1998; Henry & Campbell, 1999) that are closely associated with DGs and would support the mechanical resistance to the over-expansion of the SL.

Gene mutations of cardiac F-actin, Dys, each SG and laminin α2 in addition to lamin A/C cause DCM in human cases as the chief symptoms or partial signs (Fadic et al., 1996; Cox & Kunkel, 1997; Olson et al., 1998; Fatkin et al., 1999; Barresi et al., 2000; Tsubata et al., 2000; Politano et al., 2001; Seidman & Seidman, 2001). A gene defect and the corresponding protein disruption in one of the DAP

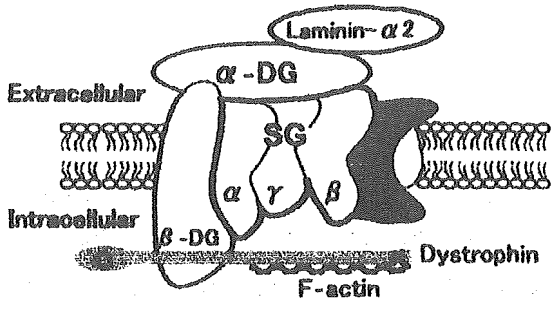

Fig. 1. A potential localization of dystrophin-associated proteins (DAPs). Mutations in DAP, which cause DCM in human cases, are shown in red characters. SG, sarcoglycan; DG, dystroglycan.

components commonly induce muscle degeneration (Seidman & Seidman, 2001), leading to cardiomyopathy or muscular dystrophy in humans (Ortiz-Lopez et al., 1997; Li et al., 1999).

In this review, we introduce a novel scheme that we assessed in 3 HF models described below. (I) Hereditary model with DCM hamsters and its gene therapy (Kawada et al., 2001, 2002; Toyo-oka et al., 2004), (II) acquired HF after high-dose administration of isoproterenol (Isp) in rats (Xi et al., 2000), and (III) chronic HF after the coronary ligation in rats (Yoshida et al., 2003).

3. Animal model of heart failure

It should be noted that an animal model is suitable for exactly evaluating the cause and following the process of diseases. The merit of naturally occurring sickness would be substantiated by the facts that the same gene mutation is documented in human patients after a candidate gene is identified in hereditary animal models. DCM is the representative model, since the δ-SG gene is missing in the BiO 14.6 and TO-2 hamster strains (Nigro et al., 1997; Sakamoto et al., 1997) and point mutations in the same gene have been reported in human families with DCM and sudden death that required heart transplantation in young patients (Tsubata et al., 2000).

Transgenic animals are very meaningful for the evaluation of the pathogenesis of variable diseases. Mice lacking SG genes effectively model human mutations leading to CM and muscular dystrophy (for review, see Lapidos et al., 2004).

3.1. Hereditary model of dilated cardiomyopathy

Animal models are of significance for both understanding the pathological mechanisms and developing new treatments (Toyo-oka et al., 2002). The CM hamster is a valuable model of human hereditary case (Homburger et al., 1962). The BIO 14.6 strain shows hypertrophic cardiomyopathy (HCM) followed by DCM (Bajusz et al., 1956; Homburger et al., 1962; Sakamoto et al., 1997), while the TO-2 strain demonstrates DCM from onset (Sakamoto et al., 1997). In the BIO 14.6 myocardium, both the β- and δ-SG proteins are missing, but both α- and γ-SG are weakly and heterogeneously expressed in cardiomyocytes in the early stages of HF. In contrast, the TO-2 strain almost loses all 4 SGs from the onset (Sakamoto et al., 1997; Kawada et al., 1999). Accordingly, the same δ-SG gene mutation causes different phenotypes and leaves a significant question to be resolved. In these strains, various pathological and physiological features have been reported, including oncosis, apoptosis, and necrosis of myocardial cells and interstitial fibrosis (Bajusz et al., 1956; Homburger et al., 1962; Jasmin & Eu, 1979; Toyo-oka et al., 2002).

Another benefit of TO-2 hamsters is the usefulness for developing gene therapy. We have succeeded in the rescue of DCM in TO-2 hamsters, using recombinant adeno-associated virus (rAAV) vector-mediated gene transduction in vivo with normal δ-SG (Kawada et al., 2001, 2002) and found that DAPs play an important role during the progression of advanced HF. Although hereditary DCM is caused by congenital loss of the δ-SG protein, the reasons for which the TO-2 strain does not show overt cardiac failure at the birth but demonstrates a slow, but steady progression of clinical symptoms have not been clarified. Similar late onset of the genetic diseases has been reported in Duchenne type muscular dystrophy (for review, see Blake et al., 2002) and Huntington's ataxia (for review, see Bates, 2003). To verify our scheme that muscular dystrophy-like lesions in cardiac muscle may lead to advanced HF, we conducted the following comprehensive studies on the progression of HF.

3.1.1. Alterations of hemodynamics and myocardial contractility

We followed the time course of hemodynamic indices in cardiac catheterization (Kawada et al., 2002) and myocardial contractility in echocardiography up to the end stage. Normal F1B hamsters revealed growth-dependent changes, and both the systolic and diastolic functions were preserved throughout the experiment (Fig. 2; Toyo-oka et al., 2004). In contrast, TO-2 strain showed both the systolic and diastolic dysfunctions (Fig. 2). In echocardiography, TO-2 strain revealed a remarkable decrease of both the fractional shortening and the left ventricular ejection fraction (data not shown). This phase matched well with the marked degradation phase and the cardiac failure. These pathophysiological features are very similar to human cases with DCM.

3.1.2. Histopathological features and expression of dystrophin

Double fluoromicroscopy to simultaneously detect the Dys disruption and sarcolemma (SL) fragility in situ during the HF progression age-dependently revealed 2 morphological characteristics in the same cardiomyocytes: (I) a shift or translocation of Dys from SL to myoplasm and (II) leaky SL to the exogenously applied Evans blue (EB) dye (Toyo-oka et al., 2004).

Western blotting of the whole myocardial homogenate without fractionation that was favorable for detecting degradation at cellular level showed characteristic findings with a specific antibody to the rod domain of Dys (Fig. 3A; Toyo-oka et al., 2004). Normal F1B hearts preserved the amount of Dys throughout life. The DCM hearts from the TO-2 strains, however, demonstrated extra-bands between 200 and 60 kDa (Fig. 3A). The densitometry revealed that Dys at 430 kDa started to decline at the beginning of HF (Fig. 2) and was markedly reduced during the progression to the advanced stage (Fig. 2), while the intensity at 60-kDa

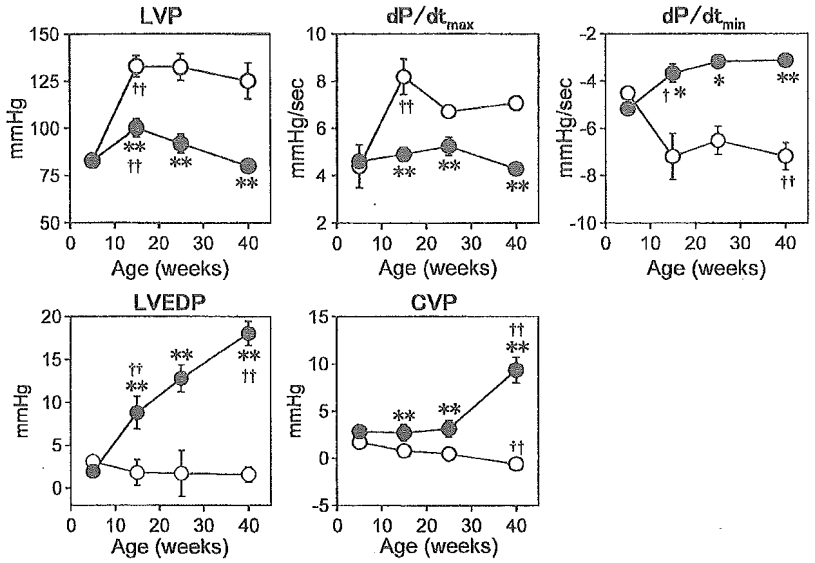

Fig. 2. Cardiac hemodynamics along progression of heart failure: left ventricular pressure (LVP), maximum dexivative of LVP (dP/dt_{max}), minimum derivative of LVP (dP/dt_{min}), the left ventricular end-diastolic pressure (LVEDP) and central venous pressure (CVP) in normal F1B strain (open circle) and TO-2 strain hamsters (closed circle). ** Indicates the significant difference, compared with the F1B strain at $P < 0.01$. † and †† also denote the significant difference, compared with the preceding age $P < 0.05$ and $P < 0.01$, respectively.

fragment increased as a mirror image to Dys (Fig. 3B). The period when the drastic cleavage occurred completely matched with the phase when the Dys translocation became evident and the animals started to die of the congestive HF (Kawada et al., 2002; Toyo-oka et al., 2004).

Surprisingly, the amount of Dys or its cleaved 60-kDa fragment in TO-2 animals very closely correlated with the homodynamic indices along the progression of HF. The Dys amount was related to the systolic index positively and to the diastolic parameters negatively (Toyo-oka et al., 2004). Very close regression coefficients between the amount of Dys and the systolic or diastolic performances support the role of Dys in transmitting the force developed through the actin–myosin cross-bridges to the extracellular matrix. It is also noteworthy that no correlation between the amounts of Dys and the maximum derivative of the left ventricular pressure (LVP) or the minimum derivative of LVP also supports no involvement of Dys in Ca^{2+} handling (Ebashi et al., 1976) or the energetics of cardiac muscle cells (Toyo-oka et al., 1992).

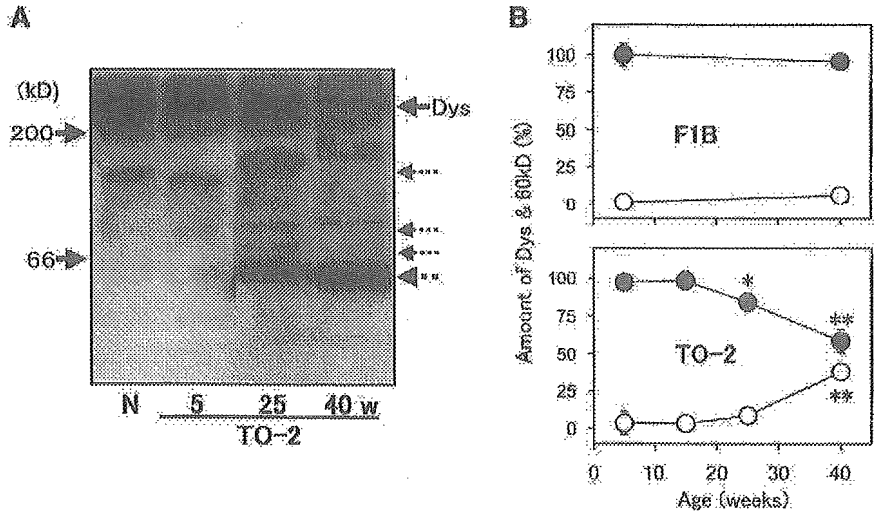

Fig. 3. Cleavage and reduction of cardiac dystrophin (Dys) during DCM progression in hamsters. (A) Normal (N, F1B strain) or DCM (TO-2 strain) hamsters at 5, 25 and 40 weeks of age (w). A solid arrow at 430 kDa and several dotted arrows denote the original Dys and its degradation products, respectively. (B) Time course of the density of immunoreactive bands specific to the rod domain of Dys at 430 kDa (closed circle) and 60 kDa (open circle) in both normal (F1B) and DCM (TO-2) strain hamsters. * and ** indicate significant differences, compared with the preceding age at $P < 0.05$ and $P < 0.01$, respectively.

3.1.3. In vivo gene transduction in dilated cardiomyopathy hamsters

Gene therapy is promising for the treatment of causative hereditary DCM, when the responsible gene is identified. Both the limited and transient expression after in vivo gene transfer precludes a functional evaluation of transduced hearts (Kawaguchi et al., 1997; Kawada et al., 1999). We examined the long-term effect of gene delivery using the rAAV vector (Kawada et al., 2001, 2002). This vector is nonpathogenic (Xiao et al., 1996; Svensson et al., 1999), long-lasting, and has been approved for therapy of human patients with cystic fibrosis (Wagner et al., 1998) or hemophilia B (Kay et al., 2000).

It should be stressed that the δ-SG gene transduction of TO-2 protected cardiomyocytes from SL instability in situ, because the EB entry escaped in cardiomyocytes transduced by the δ-SG gene (Kawada et al., 2002). Even local expression of the δ-SG transgene improved cardiac dysfunction and prognosis (Fig. 4, δ-SG; Toyo-oka et al., 2004). Furthermore, this gene therapy also ameliorated the Dys translocation in the same cardiomyocytes as the δ-SG expressing cells for up to 35 weeks (Fig. 4, Dys). In contrast, nontransfected cells showed translocation of Dys in the same sample (indicated by arrows in Fig. 4, Dys). These findings distinctly eliminate the possibility that the Dys disruption resulted from an epiphenomenon of HF, because the Dys translocation was restricted to cardiomyocytes that did not express the δ-SG transgene in the same observation field. We conclude that SL degeneration would disrupt the DAP leading to the advanced HF and that present gene therapy would rescue the deterioration of DAP by the transduction of δ-SG.

3.2. Acquired model of heart failure with catecholamine toxicity

Myocardial damage has been reported in human patients who received a large dose of Isp under certain circumstances (Lockett, 1965). In addition, plasma catecholamine levels increase in patients with advanced HF (Thomas & Marks, 1978), and β-adrenergic agonists deteriorate both cardiac function and prognosis of patients. In contrast, several β-blockers have been shown to improve mortality and morbidity (Gottlieb et al., 1998; Packer et al., 2001; Poole-Wilson et al., 2003). A toxic dose of Isp to normal rats causes acute HF and morphological disorganization (Kahn et al., 1969). These results suggest that stimulation of the sympathetic nervous system contributes to the progression of HF (for review, see Lohse et al., 2003).

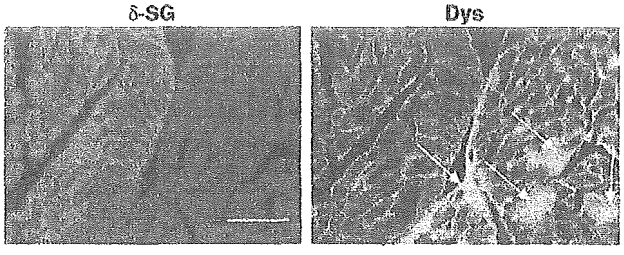

Fig. 4. Double immunostaining of δ-sarcoglycan (SG, RITC) and dystrophin (Dys, FITC) of TO-2 hamster hearts 35 weeks after local δ-SG gene transfection in vivo. Arrows indicate cardiomyocytes where Dys was translocated from the SL to the myoplasm (Bar 40 μm).

3.2.1. Catecholamine and heart failure

The actions of β-agonists are mediated through cyclic adenosine monophosphate (cAMP)-dependent protein kinase (A-kinase) system (Huston & Krebs, 1968). This results in phosphorylation of myocardial proteins, including voltage-dependent Ca^{2+} channels, phospholamban, inhibitory subunit of troponin (TN)-I, and cAMP-responsive element-binding protein, and modulates myocardial function and gene expression (for review, see Lohse et al., 2003). The major pathway during β-agonist stimulation is cAMP-dependent activation of the A-kinase in short time. Elevated intracellular Ca^{2+} levels after β-agonist stimulation may partially mediate the hypertrophic remodeling in long term (Engelhardt et al., 2001). Indeed, common observations in various models of cardiac hypertrophy confirmed the alteration of Ca^{2+} handling within cardiomyocyte, which leads to a pronounced elevation in Ca^{2+} influx (Jacob et al., 1983; Engelhardt et al., 2001).

3.2.2. Proteases activated by isoproterenol

As early as 1968, 2 groups identified muscle-endogenous A-kinase activating factor (KAF) as a proteolytic enzyme (Drummond & Duncan, 1968; Huston & Krebs, 1968). KAF was later termed as Ca^{2+}-activated neutral protease (CANP) or calpain. Catecholamine toxicity would result from irreversible and uncontrolled up-regulation of A-kinase activity and energy depletion (Toyo-oka et al., 1992).

Ca^{2+}-sensitive proteases, calpain family in myoplasm, may be involved in the biochemical and functional changes associated with Isp-induced cardiac damage. Caseinolytic activity in the left ventricle is found to increase over control cardiac muscle after Isp administration (Arthur & Belcastro, 1997). The elevated intracellular Ca^{2+} levels following β-adrenergic receptor stimulation increase calpain activity (Iizuka et al., 1991) that may also require membrane phospholipids for the activation (Saido et al., 1992). The β-receptor coupled Gs proteins directly gate the Ca^{2+} channels on SL (for review, see Endoh, 1995) and increases local Ca^{2+} levels. The SL in proximity to the β-receptor could, therefore, supply an ideal location for calpain activation in response to Isp. Indeed, one of the schemes to explain how intracellular calpain is activated proposes that the mechanism is a membrane- and, accordingly, phospholipid-associated event (Saido et al., 1992). In addition to calpains, other lysosomal protease(s) might be also involved in HF, because the administration of Isp induces myocardial infarction followed by the increasing activity

of cathepsins in rats (Ravichandran et al., 1991; Macickova et al., 1999).

3.2.3. Acquired heart failure after isoproterenol administration

We evaluated the morphological and biological effects of Isp in rats (Xi et al., 2000). A toxic dose of Isp induced the following phenomena. (I) Immunoreactive Dys detected by the specific antibody was heterogeneously distributed in both the SL and the myoplasm (Fig. 5A, Dys), while control rat hearts showed a clear staining selectively in the SL. In contrast, δ-SG remained localized in the SL not only in control but also in Isp-treated rats (Fig. 5A, δ-SG). (II) Western blotting revealed the time-dependent cleavage of Dys (Fig. 5B, left), while δ-SG was not hydrolyzed at all (Fig. 5B, right). (III) Very interestingly, the degraded fragments of Dys after Isp treatment revealed the similar size in DCM hamsters at the advanced stage (Toyo-oka et al., 2004). (IV) Confocal microscopy of cardiomyocytes showed EB uptake. The Dys shift was restricted to EB-positive cells (Toyo-oka et al., 2004). These results indicate that the Isp treatment simultaneously caused cleavage of Dys, but not δ-SG, and the fragility of SL as an acute event up to 16 hr. It should be noted that both the cleavage and shift of Dys in addition to the EB entry was documented in TO-2 hearts as a long term up to 40 weeks.

3.3. Heart failure secondary to myocardial infarction

3.3.1. Chronic heart failure after coronary ligation in rats

We measured hemodynamic indices and immunologically analyzed DAP in the chronic HF model secondary to old myocardial infarction (OMI) in rats (Yoshida et al., 2003). The LVP, the maximum derivative of the LVP, the minimum derivative of LVP and the aortic pressure were reduced, compared to the sham operation group at the chronic stage after the coronary ligation, whereas the left ventricular end-diastolic pressure was extremely increased as high as 30 mmHg (Fig. 6). Western blotting in the viable myocardium indicated that both Dys and α-SG were remarkably reduced but the δ-SG was completely preserved (Fig. 7).

3.3.2. Acute heart failure after myocardial ischemia in dogs

Toyo-oka and Ross (1981) followed the time course of Ca^{2+} sensitivity of natural actomyosin (NAM) from the area of acute myocardial infarction (AMI) after the coronary artery ligation in dogs. NAM from the intact tissue showed normal superprecipitation and normal Ca^{2+} sensitivity. Four hours after coronary ligation, Ca^{2+} sensitivity was lowered only in the endocardial half of AMI region; it was markedly decreased both in the epicardial and endocardial halves at 6 hr and completely lost at 24 and 48 hr. A superprecipitation response was, however, demonstrated in all samples,

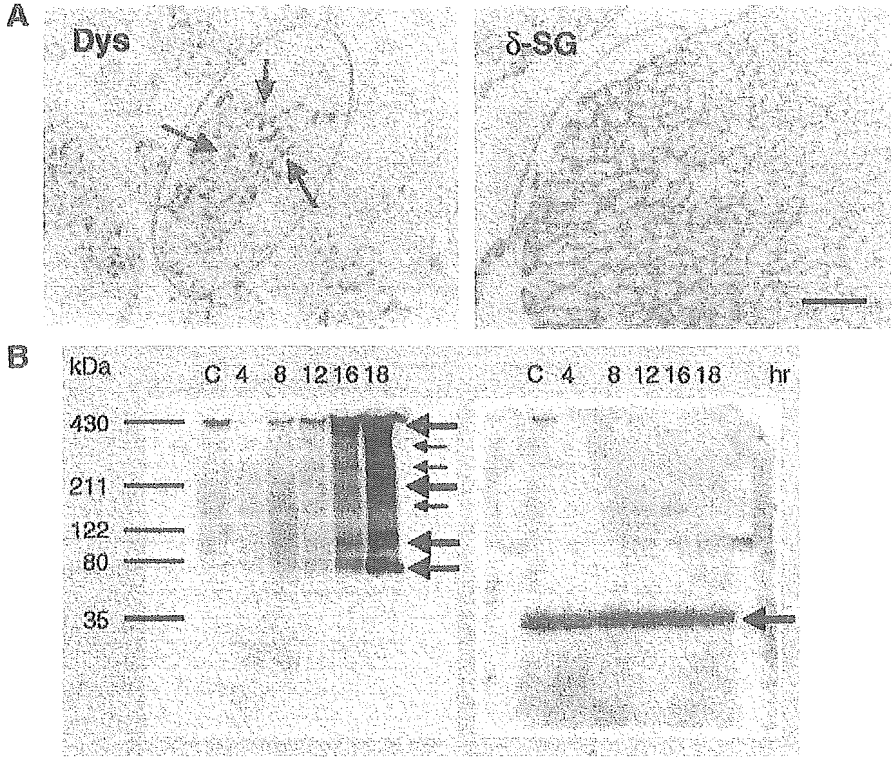

Fig. 5. Translocation and cleavage of dystrophin (Dys) and δ-sarcoglycan (SG) after the administration of isoproterenol (Isp) high dose. (A) Dys but not δ-SG shifted from sarcolemma to myoplasm (Dys, arrows in an oval) after Isp treatment (Bar 50 μm). (B) By Western blotting, Dys cleaved time-dependently (left panel, arrows). In contrast, δ-SG was not hydrolyzed at all (right panel, arrow). hr, hour after the Isp administration.

indicating that both myosin and actin preserved their functions in the course of AMI.

With SDS-PAGE, NAM from the AMI region revealed moderate decreases in TN-T and TN-C and a drastic reduction in TN-I, resulting in the formation of extra bands of low molecular weights. These results suggest that degradation of TN subunits occurs as early as 4 hr and from the endocardial half of AMI region. This degradation may be caused by protease(s) that preferentially degrade the regulatory proteins among myofibrillar proteins (Toyo-oka & Ross, 1981).

Other in vitro evidence that calpain might be responsible for the proteolysis of TN-I was derived from the result that purified TN-I was easily degraded by the isolated calpain 2 (Toyo-oka & Masaki, 1979). Phosphorylated cardiac TN-I with A-kinase was more preferentially hydrolyzed by calpain 2 than the nonphosphorylated one (Toyo-oka, 1982). Considering the clinical setting of AMI where serum catecholamine levels are extremely increased (Horvat et al., 1972), the TN degradation might be accelerated during the pathological progression.

3.3.3. Chronic heart failure after old myocardial infarction in humans

The preferential breakdown of TN-I among sarcomeric proteins would explain the clinical diagnostic value of serum TN-I levels after the onset of AMI. TN-I is more specific than total creatine phosphokinase activity or even its MB-isoform. The TN-I level was useful for early risks stratification in unstable coronary artery disease (Luscher et al., 1997). Elevated levels of TN-T were also associated with an increased risk of cardiac death at 30 days. TN-I levels

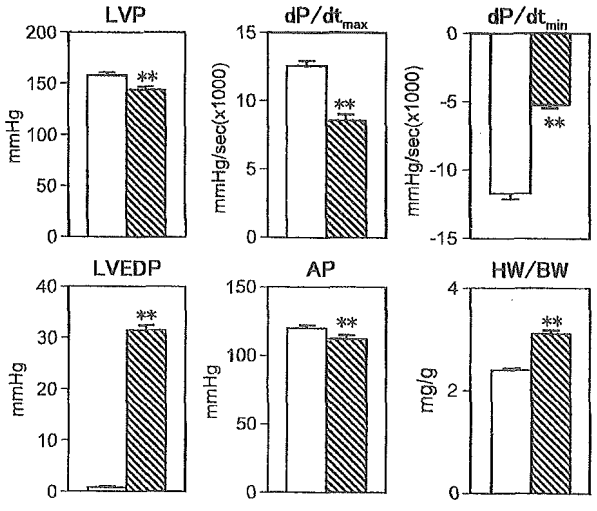

Fig. 6. Cardiac hemodynamic and physical indices of the sham and coronary ligation rats at the 8th weeks after the operation. Left ventricular pressure (LVP), maximum derivative of LVP (dP/dt_{max}), minimum derivative of LVP (dP/dt_{min}), the left ventricular end-diastolic pressure (LVEDP), aortic pressure (AP) and heart weight/body weight ratio (HW/BW) in sham operation (open columns) and coronary ligation (hatched columns) rats. ** Indicates a significant difference, compared with the sham operation group at $P < 0.01$.

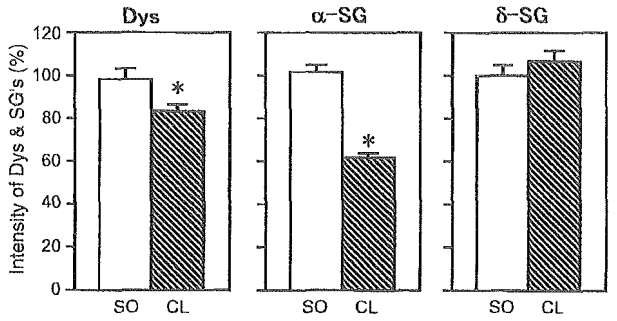

Fig. 7. Expression amounts of the dystrophin (Dys), α-sarcoglycan (SG) and δ-SG band in the viable left ventricular free wall of the sham (SO) and coronary ligation (CL) rats at the 8th weeks after the operation. * Indicates a significant difference, compared with the sham operation group at $P < 0.05$.

similarly indicate increased risk of cardiac death (Luscher et al., 1997). Furthermore, the serum level of cardiac TN-I may predict the prognosis of advanced HF, irrespective of its origins (Antman et al., 1996; Horwich et al., 2003).

4. Protein turnover under pathological conditions

The expression levels of proteins are dependent on the dynamic equilibrium between the protein synthesis and degradation rates. The degradation in several HFs described above would suggest the enhanced activation of proteolytic enzymes in situ and/or the contribution of proteasomes. The counterpart protein synthesis of each component of DAP has not been precisely elucidated, and very few papers are currently available that measure expression levels of mRNA. Furthermore, the level of mRNA does not always correlate with the amount of expressed proteins.

4.1. Cleavage of myocardial proteins in human heart failure and animal models

Towbin's group has reported the disruption of Dys in patients with end-stage DCM and ischemic CM (Vatta et al., 2002). We also demonstrated that the cleavage of Dys as detected in human DCM of unidentified etiology in cardiac transplantation (Fig. 8A; Toyo-oka et al., 2004). The topological shift of Dys was also documented in samples of the advanced stage of DCM (unpublished data). Accordingly, the translocation was common to both animals (Fig. 3) and humans with DCM. The distinct relationship was found between the amount of Dys and the survival rate of DCM hamsters over the age (Fig 8B; Kawada et al., 2002; Toyo-oka et al., 2004).

The characteristics of 3 models and human cases with advanced HF are summarized in Table 1. Myocardial Dys was decreased in all animal models (Yoshida et al., 2003; Toyo-oka et al., 2004) and humans (Toyo-oka et al., 2004). TO-2 hamsters as a hereditary HF model revealed the heterogeneous reduction of some, but not all, components of DAPs (Sakamoto et al., 1997; Kawada et al., 1999). δ-SG was not

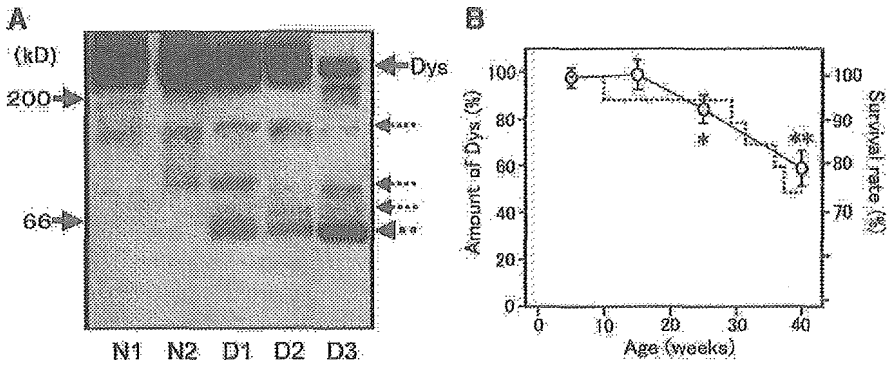

Fig. 8. (A) Cleavage and reduction of cardiac dystrophin (Dys) in normal humans (N1 and N2) and patient with DCM (D1, D2 and D3) at the time of cardiac transplantation. A solid arrow at right-hand side of the panel (430 kDa) and dotted arrows denote the original Dys and its degradation products, respectively. (B) Time course of the density of immunoreactive bands specific to the rod domain of Dys at 430 kDa (open circle) and the survival rate (dotted line) in DCM hamsters. * and ** indicate significant differences, compared with the preceding age at $P < 0.05$ and $P < 0.01$, respectively.

identified because of the gene deletion (Sakamoto et al., 1997). In contrast, the acquired model demonstrated a decrease in α-SG, but no change in δ-SG (Xi et al., 2000, Fig. 5; Yoshida et al., 2003, Fig. 7). Intracellular Ca^{2+} levels were reported to be elevated in all of these models (for review, see Katz, 1979; Katz & Reuter, 1979; Whitmer et al., 1988; Arthur & Belcastro, 1997) and humans (Gwathmey et al., 1987). Furthermore, we have shown that expression of the δ-SG transgene in TO-2 hamsters normalized the SL permeability (Kawada et al., 2002). EB staining in cardiomyocytes of hereditary and acquired models was extensively documented, indicating the lack of SL integrity (Toyo-oka et al., 2004).

4.2. Expression of dystrophin-associated proteins under pathological conditions

There have been very few data measuring mRNA expression of Dys. Maeda et al. (2003) reported that Dys transcript in the left ventricular muscle was significantly increased after the aortic banding, driven by tissue-specific exon 1 with a muscle-specific type promoter, but not a nonmuscle type promoter (brain and Purkinje-cell type). Thus, the Dys gene was up-regulated and then the transgene expression was increased in response to cardiac hypertrophy, suggesting the compensation of Dys in maintaining SL integrity in the hypertrophic stage.

We have also documented that α-SG protein levels were greatly reduced as well in TO-2 hamster hearts (Sakamoto et al., 1997; Kawada et al., 1999) or viable tissues of infarcted myocardium in rats (Fig. 7; Yoshida et al., 2003). In addition, α-SG was the most susceptible among DAPs to the proteolysis by isolated calpain 2 in vitro (Fig. 9; Yoshida et al., 2003). However, dot hybridization analyses revealed no increase in mRNA of each DAP component under these HF conditions (data not shown), suggesting that compensatory expression did not occur in the case of DAP. Similar results were reported by Straub et al. (1998), though they did not employ the TO-2 strain that shows overt HF from the onset but the BIO 14.6 strain that initially demonstrates cardiac hypertrophy followed by advanced HF at the end stage (Whitmer et al., 1988; Kawada et al., 1999).

Table 1
Characteristics of employed 3 models and human advanced heart failure

Models	TO-2	OMI	Isp	Human	In vitro susceptibility to calpain 2
Etiology	Hereditary	Acquired		Unidentified	
Progression	Chronic	Chronic	Acute	Chronic	
Dystrophin	↓ ↓	↓	↓ ↓	↓ ↓	+
DAP complex					
α-SG	↓	↓	↓		++
β-SG	↓	→	↓	ND	++
γ-SG	↓	→	→		–
δ-SG	Null	→	→		–
$[Ca^{2+}]_i$	↑ ↑	↑	↑ ↑	↑ ↑	
EB staining	+	+	+	ND	

OMI = old myocardial infraction; Isp = isoproterenol; DAP = dystrophin-associated proteins; SG = sarcoglycan; Dys = dystrophin; $[Ca^{2+}]_i$ = intracellular Ca^{2+}; EB = Evans blue; ND = no determined.

5. Contribution of calpains to the induction of heart failure

What is the factor responsible for the Dys disruption in these pathological conditions? The limited hydrolysis of

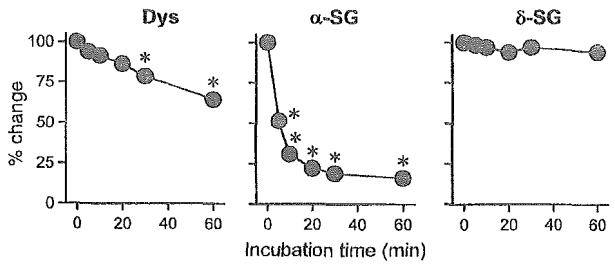

Fig. 9. Time course of cleavage of dysirophin (Dys), α-sarcoglycan (SG) and δ-SG in the isolated sarcolemma fraction with purified calpain 2 from porcine heart. * Indicates a significant difference, compared with the preincubation value (0 min) at $P < 0.05$.

Dys in HF strongly suggests a contribution of proteases under the elevation of intracellular Ca^{2+}. We propose that the Ca^{2+}-activated neutral protease (calpain 1 and/or 2) as one of the candidates, because cardiomyocytes contain an appreciable amount (Toyo-oka et al., 1978) and intracellular Ca^{2+} handling is modified in failing hearts (for review, see Katz, 1979; Katz & Reuter, 1979; Gwathmey et al., 1987; Whitmer et al., 1988; Gavin & Belcastro, 1997). Calpain belongs to a nonlysosomal protease family containing a cysteine residue in the active site and has an absolute dependence on Ca^{2+} for catalytic activity (Ishiura et al., 1978). The substrates for calpain involve several proteins, including myofibrillar proteins such as TN-T and -I in both skeletal muscle (Dayton et al., 1981; Ohtsuki et al., 1984) and cardiac muscle (Toyo-oka & Masaki, 1979).

5.1. Isoforms of calpain and the activation mechanism

At present, more than 15 isoforms of calpain have been reported in a variety of tissues and species (for review, see Goll et al., 2003). Ubiquitous calpain is composed of 2 distinct isoforms, calpain 1 (μ-CANP) and calpain 2 (m-CANP). Both calpains are similar in substrate specificity but differ in their requirements for Ca^{2+}; calpain 1 is activated by micromolar intracellular Ca^{2+}, whereas calpain 2 requires millimolar intracellular Ca^{2+} for the maximal activation (Mellgren, 1980; for review, see Suzuki et al., 1995). Both calpain 1 and 2 degrade cytoskeletal proteins, membrane receptors (Saido et al., 1994), and Dys (Fig. 9; Yoshida et al., 2003) when activated. Thus, during cardiac ischemia, the increased level of myocardial Ca^{2+} would activate the calpains, causing damage to myocardial proteins (Yoshida et al., 1995), and lead to myocyte death in the cell level and, consequently, to loss of myocardial structure and function in organ level (Toyo-oka, 1982; Toyo-oka et al., 1982, 1985). Indeed, several data suggest the involvement of the calpains in myocardial ischemia–reperfusion injury (Toyo-oka et al., 1991; Yoshida et al., 1995), myocardial stunning (Matsumura et al., 1993), cardiac hypertrophy (Arthur & Belcastro, 1997), and myocardial infarction (Sandmann et al., 2001, 2002; Yoshida et al., 2003).

5.2. Stoichiometry between calpain and calpastatin

Neither specific inhibitors of calpain nor calpain-knockout animals are available to test this hypothesis. Calpastatin has been shown to completely inhibit proteolytic actions of both calpain 1 and 2 at an equimolar stoichiometry (Suzuki et al., 1987). In OMI rats the protein level of calpain 2 also increased in viable left ventricles after the coronary ligation. However, calpastatin levels did not change. Accordingly, calpain levels became dominant relative to calpastatin levels (Yoshida et al., 2003).

Although these data have a significant meaning for the pathological contribution of calpain, much care should be paid for the exact evaluation as follows. (I) Both calpain 1 and 2 exist in the myoplasm and weakly, but significantly, bind to the SL (for review, see Suzuki et al., 1995). For the exact assay of calpain activity, fractionation after homogenization may not exactly reflect the precise localization of each protease. (II) Both calpains and their counterpart, calpastatin, coexist in the myoplasm and SL. Without a distinct isolation of each calpain from calpastatin, the apparent, but not net, activities of calpain isoforms would not represent an in vivo function, because both enzymes differ in their regional and temporal activation within the infarcted myocardium (Sandmann et al., 2001, 2002). (III) The actual proteolytic activity should be determined in parallel with hydrolytic activity using synthetic fluorogenic substrate that is much more sensitive and accordingly easier to assay, since cardiac tissue endogenously contains several hydrolases that have not been exactly specified yet (Ikeda et al., 1986).

5.3. Endogenous substrates for calpains among dystrophin-associated proteins

To examine the proteolysis of Dys and SGs by calpain 2 in vitro, we used an SL-enriched fraction. Purified calpain degraded Dys and α- and β-SGs in the presence of Ca^{2+} in a time-dependent manner. However, δ-SG was not significantly hydrolyzed (Fig. 9 and Table 1; Yoshida et al., 2003). It should be noted that the isolated fraction is often contaminated by endogenous protease(s) including calpain(s) and spontaneously hydrolyzed without adding exogenous calpain. We have defined calpain as the protease that satisfies following 3 criteria: (I) most active at neutral pH; (II) sensitive to mM and μM Ca^{2+} in case of calpain 2 and calpain 1, respectively; and (III) completely inhibited at 100 μM leupeptin and/or antipain (Toyo-oka et al., 1978). These results suggest that calpain 2 mainly contributes to the cleavage of Dys.

6. A novel paradigm for the progression of advanced heart failure

Cardiac muscle repeats contraction and relaxation throughout its life and myocardial SL should be more resistant to the expansion and shrinkage cycling in cardiac muscle contraction than SL of skeletal muscle. Missing a component of DAP is not lethal, but it may be needed to maintain membrane integrity and the normal life expectancy. However, continuous but gradual leakage of SL to Ca^{2+} in addition to the Ca^{2+} entry during slow inward currents would elevate intracellular Ca^{2+} levels in DCM (Gwathmey et al., 1987). Ca^{2+} handling in DCM heart might be distinctly different from HCM heart (Whitmer et al., 1988).

In case of point mutation of DAP genes that has been particularly reported in Dys (Cohen & Muntoni, 2004) or δ-SG (Tsubata et al., 2000) to cause a replacement of amino acid, 2 possibilities leading to the advanced HF would be raised. First, higher structure of the transgene is changed

and results in "loss of function" to bind with β-DG at C-terminal or actin at N-terminal in the case of Dys or to make a complex with counterpart of other SGs (Sakamoto et al., 1997). Second, the replacement does not cause a harmful effect on the function of transgene per se, but may be susceptible to endogenous protease(s) or proteasome(s). It may be attractive to assume that the mutated DAP protein would be more easily hydrolyzed with the mechanism to exclude foreign protein by the house keeping protease(s).

Furthermore, an acquired case in mice with myocarditis after enterovirus infection shows DCM-like symptoms secondary to the selective cleavage of Dys and in addition to α-SG by protease 2A translated from the virus genome (Badorff et al., 1999). Chronic HF secondary to OMI also demonstrated that both Dys and α-SG were remarkably reduced in viable myocardium, whereas δ-SG was completely preserved (Fig. 7; Yoshida et al., 2003). In case of viable tissue in OMI, high-energy phosphates are depleted and inorganic phosphate is accumulated in myoplasm (Toyo-oka et al., 1992). After that, the rate of active transport of Ca^{2+} through SL or sarcoplasmic reticulum via the respective Ca^{2+}-ATPase is lowered. The isometric tension did not parallel to the consumption of ATP under the condition of increased phosphate and H^+ (Takayasu et al., 1990) and may result in the vicious cycle of energy depletion and loss of myocardial contractility. A toxic dose of Isp would induce Ca^{2+} overload through activation of L type Ca^{2+} channels. All these pathological settings would elevate Ca^{2+} in the myoplasm.

On the pathogenesis of DCM, Sonnenblick's group raised "angiogenic theory (1982)" that coronary spasm in DCM hamster is responsible for the induction of myocardial cell degradation (Factor et al., 1982). This scheme was further supported by the transgenic mice where β-, δ-, and γ-SG genes were knocked out and microcirculation in these mice was disturbed (Coral-Vazquez et al., 1999; Cohn et al., 2001; Wheeler et al., 2004). To establish the idea, more precise evaluations would be needed, checking the following several points: (I) whether necrotic lesion is detected along the coronary arteries; (II) to prevent the coronary spasm using pharmaceutical drugs, more potent and specific agent should be employed, not nicorandil, a K^+ channel opener or verapamil, phenylalkylamine-derived Ca^{2+} entry blocker that preferentially inhibits L-type Ca^{2+} channels in cardiomyocytes (Toyo-oka & Nayler, 1996), but nitrate or dihydropyridine-derived Ca^{2+} antagonists that mainly block Ca^{2+} entry in coronary smooth muscle cells.

We propose a novel scheme for the progression of 3 models of HF to the advanced stage (Fig. 10). In these models, substantial activation of calpains following the elevated intracellular Ca^{2+} would induce the specific proteolysis of Dys in addition to α-SG as is similar to the hydrolysis of talin during platelet aggregation (Toyo-oka et al., 1989). After that, SL integrity would be lost, and SL would be permeable to extracellular Ca^{2+} and be unable to maintain the physiological Ca^{2+} gradient of through the SL.

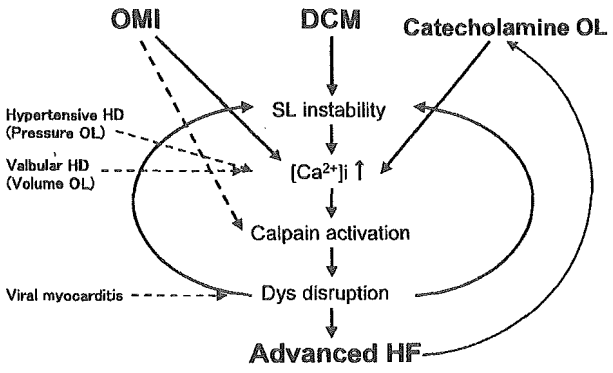

Fig. 10. Scheme for the progression of heart failure (HF) in three animal models and human diseases to the advanced stage. OMI, old myocardial infarction; DCM, dilated cardiomyopathy; OL, overload; SL, sarcolemma; Dys, dystrophin; $[Ca^{2+}]_i$, intracellular Ca^{2+}; HD, heart disease; HF, heart failure.

The vicious cycle would result in the disruption of Dys and myocardial cell death.

7. Conclusion

We summarize a scheme of the progression of 3 animal models of HF and human diseases to the advanced stage (Fig. 10). These results of HF, irrespective of the hereditary or acquired origin with an acute or chronic process, indicate a vicious cycle characterized by (I) an increased SL permeability, (II) preferential activation of calpains over calpastatin, and (III) a shift and cleavage of Dys, all of which would lead to advanced HF. Gene therapy using efficient and long-lasting rAAV vectors may provide a new strategy for the causative or symptomatic treatment of HF.

Note

During the printing process of this manuscript, a new paper has appeared in *Cardiovasc. Res.* 65: 356–65, 2005, written by Takahashi et al., Effects of ACE inhibitor & AT1 blocker on dystrophin-related proteins & calpain in failing heart.

Acknowledgments

This study was financially supported by the Ministry of Education, Science, Sports, and Culture, Japan, and the Translational Project in Ministry of Welfare and Labor, Japan, the Mitsubishi Research Foundation, and the Motor Vehicle Foundation.

References

Antman, E. M., Tanasijevic, M. J., Thompson, B., Schactman, M., McCabe, C. H., Cannon, C. P., et al. (1996). Cardiac-specific troponin I levels to

predict the risk of mortality in patients with acute coronary syndromes. *N Engl J Med 335*, 1342–1349.

Arthur, G. D., & Belcastro, A. N. (1997). A calcium stimulated cysteine protease involved in isoproterenol induced cardiac hypertrophy. *Mol Cell Biochem 176*, 241–248.

Badorff, C., Lee, G. H., Lamphear, B. J., Martone, M. E., Campbell, K. P., Rhoads, R. E., et al. (1999). Enteroviral protease 2A cleaves dystrophin: evidence of cytoskeletal disruption in an acquired cardiomyopathy. *Nat Med 5*, 320–326.

Bajusz, E., Baker, J. R., & Nixon, C. W. (1956). Spontaneous, hereditary myocardial degeneration and congestive heart failure in a strain of Syrian hamsters. *Ann N Y Acad Sci 156*, 105–129.

Barresi, R., Di Blasi, C., Negri, T., Brugnoni, R., Vitali, A., Felisari, G., et al. (2000). Disruption of heart sarcoglycan complex and severe cardiomyopathy caused by β-sarcoglycan mutations. *J Med Genet 37*, 102–107.

Bates, G. (2003). Huntingtin aggregation and toxicity in Huntington's disease. *Lancet 361*, 1642–1644.

Blake, D. J., Weir, A., Newey, S. E., & Davies, K. E. (2002). Function and genetics of dystrophin and dystrophin-related proteins in muscle. *Physiol Rev 82*, 291–329.

Cohen, N., & Muntoni, F. (2004). Multiple pathogenetic mechanisms in X-linked dilated cardiomyopathy. *Heart 90*, 835–841.

Cohn, R. D., Durbeej, M., Moore, S. A., Coral-Vazquez, R., Prouty, S., & Campbell, K. P. (2001). Prevention of cardiomyopathy in mouse models lacking the smooth muscle sarcoglycan–sarcospan complex. *J Clin Invest 107*, R1–R7.

Coral-Vazquez, R., Cohn, R. D., Moore, S. A., Hill, J. A., Weiss, R. M., Davisson, R. L., et al. (1999). Disruption of the sarcoglycan–sarcospan complex in vascular smooth muscle: a novel mechanism for cardiomyopathy and muscular dystrophy. *Cell 98*, 465–474.

Cox, G. F., & Kunkel, L. M. (1997). Dystrophies and heart disease. *Curr Opin Cardiol 12*, 329–343.

Dayton, W. R., Schollmeyer, J. V., Lepley, R. A., & Cortes, L. R. (1981). A calcium-activated protease possibly involved in myofibrillar protein turnover. Isolation of a low-calcium-requiring form of the protease. *Biochim Biophys Acta 659*, 48–61.

Drummond, G. I., & Duncan, L. (1968). On the mechanism of activation of phosphorylase b kinase by calcium. *J Biol Chem 243*, 5532–5538.

Ebashi, S., Nonomura, Y., Toyo-oka, T., & Katayama, E. (1976). Regulation of muscle contraction by the calcium–troponin–tropomyosin system. *Symp Soc Exp Biol 30*, 349–360.

Endoh, M. (1995). The effects of various drugs on the myocardial inotropic response. *Gen Pharmacol 26*, 1–31.

Engelhardt, S., Boknik, P., Keller, U., Neumann, J., Lohse, M. J., & Hein, L. (2001). Early impairment of calcium handling and altered expression of junction in hearts of mice overexpressing the β_1-adrenergic receptor. *FASEB J 15*, 2718–2720.

Factor, S. M., Minase, T., Cho, S., Dominitz, R., & Sonnenblick, E. H. (1982). Microvascular spasm in the cardiomyopathic hamster: a preventable cause of focal myocardial necrosis. *Circulation 66*, 342–354.

Fadic, R., Sunada, Y., Waclawik, A. J., Buck, S., Lewandoski, P. J., Campbell, K. P., et al. (1996). Brief report: deficiency of a dystrophin-associated glycoprotein (adhalin) in a patient with muscular dystrophy and cardiomyopathy. *N Engl J Med 334*, 362–366.

Fatkin, D., MacRae, C., Sasaki, T., Wolff, M. R., Porcu, M., Frenneaux, M., et al. (1999). Missense mutations in the rod domain of the lamin A/C gene as causes of dilated cardiomyopathy and conduction-system disease. *N Engl J Med 341*, 1715–1724.

Gavin, D. A., & Belcastro, A. N. (1997). A calcium stimulated cysteine protease involved in isoproterenol induced cardiac hypertrophy. *Mol Cell Biochem 176*, 214–248.

Goll, D. E., Thompson, V. F., Li, H., Wei, W., & Cong, J. (2003). The calpain system. *Physiol Rev 83*, 731–801.

Gottlieb, S. S., McCarter, R. J., & Vogel, R. A. (1998). Effect of beta-blockade on mortality among high-risk and low-risk patients after myocardial infarction. *N Engl J Med 339*, 489–497.

Gwathmey, J. K., Copelas, L., MacKinnon, R., Schoen, F. J., Feldman, M. D., Grossman, W., et al. (1987). Abnormal intracellular calcium handling in myocardium from patients with end-stage heart failure. *Circ Res 61*, 70–76.

Henry, M. D., & Campbell, K. P. (1999). Dystroglycan inside and out. *Curr Opin Cell Biol 11*, 602–607.

Holt, K. H., Lim, L. E., Straub, V., Venzke, D. P., Duclos, F., Anderson, R. D., et al. (1998). Functional rescue of the sarcoglycan complex in the BIO 14.6 hamster using δ-sarcoglycan gene transfer. *Mol Cell 1*, 841–848.

Homburger, F., Baker, J. R., Nixon, C. W., & Whitney, R. (1962). Primary, generalized polymyopathy and cardiac necrosis in an inbred line of Syrian hamsters. *Med Exp 6*, 339–345.

Horvat, M., Yoshida, S., Prakash, R., Marcus, H. S., Swan, H. J., & Ganz, W. (1972). Effect of oxygen breathing on pacing-induced angina pectoris and other manifestations of coronary insufficiency. *Circulation 45*, 837–844.

Horwich, T. B., Patel, J., MacLellan, W. R., & Fonarow, G. C. (2003). Cardiac troponin I is associated with impaired hemodynamics, progressive left ventricular dysfunction, and increased mortality rates in advanced heart failure. *Circulation 108*, 833–838.

Huston, R. B., & Krebs, E. G. (1968). Activation of skeletal muscle phosphorylase kinase by Ca^{2+}: II. Identification of the kinase activating factor as a proteolytic enzyme. *Biochemistry 7*, 2116–2122.

Iizuka, K., Kawaguchi, H., & Yasuda, H. (1991). Calpain is activated by β-adrenergic receptor stimulation under hypoxic myocardial cell injury. *Jpn Circ J 55*, 1086–1093.

Ikeda, U., Toyo-oka, T., & Hosoda, S. (1986). Identification of two new calcium dependent hydrolases in the human heart. *Biochem Biophys Res Commun 136*, 773–777.

Ishiura, S., Murofushi, H., Suzuki, K., & Imahori, K. (1978). Studies of a calcium-activated neutral protease from chicken skeletal muscle: I. Purification and characterization. *J Biochem (Tokyo) 84*, 225–230.

Jacob, R., Kissling, G., Ebrecht, G., Holubarsch, C., Medugorac, I., & Rupp, H. (1983). Adaptive and pathological alterations in experimental cardiac hypertrophy. In E. Chazov, V. Saks, & G. Rona (Eds.), *Advances in Myocardiology vol. 4* (pp. 55–77). Plenum Publishing Corporation.

Jasmin, G., & Eu, H. Y. (1979). Cardiomyopathy of hamster dystrophy. *Ann N Y Acad Sci 317*, 46–58.

Jessup, M., & Brozena, S. (2003). Heart failure. *N Engl J Med 348*, 2007–2018.

Kahn, D. S., Rona, G., & Chappel, C. I. (1969). Isoproterenol-induced cardiac necrosis. *Ann N Y Acad Sci 156*, 285–293.

Katz, A. M. (1979). Role of the contractile proteins and sarcoplasmic reticulum in the response of the heart to catecholamines: an historical review. *Adv Cycl Nucleotide Res 11*, 303–343.

Katz, A. M., & Reuter, H. (1979). Cellular calcium and cardiac cell death. *Am J Cardiol 44*, 188–190.

Kawada, T., Nakatsuru, Y., Sakamoto, A., Koizumi, T., Shin, W. S., Okai-Matsuo, Y., et al. (1999). Strain- and age-dependent loss of sarcoglycan complex in cardiomyopathic hamster hearts and its re-expression by δ-sarcoglycan gene transfer in vivo. *FEBS Lett 458*, 405–408.

Kawada, T., Sakamoto, A., Nakazawa, M., Urabe, M., Masuda, F., Hemmi, C., et al. (2001). Morphological and physiological restorations of hereditary form of dilated cardiomyopathy by somatic gene therapy. *Biochem Biophys Res Commun 284*, 431–435.

Kawada, T., Nakazawa, M., Nakauchi, S., Yamazaki, K., Shimamoto, R., Urabe, M., et al. (2002). Rescue of hereditary form of dilated cardiomyopathy by rAAV-mediated somatic gene therapy: amelioration of morphological findings, sarcolemmal permeability, cardiac performances, and the prognosis of TO-2 hamsters. *Proc Natl Acad Sci U S A 99*, 901–906.

Kawaguchi, H., Shin, W. S., Wang, Y., Inukai, M., Kato, M., Matsuo-Okai, Y., et al. (1997). In vivo gene transfection of human endothelial cell nitric oxide synthase in cardiomyocytes causes apoptosis-like cell death.

Identification using Sendai virus-coated liposomes. *Circulation 95*, 2441–2447.

Kay, M. A., Manno, C. S., Ragni, M. V., Larson, P. J., Couto, L. B., McClelland, A., et al. (2000). Evidence for gene transfer and expression of factor IX in haemophilia B patients treated with an AAV vector. *Nat Genet 24*, 257–261.

Krum, H., & Gilbert, R. E. (2003). Demographics and concomitant disorders in heart failure. *Lancet 362*, 147–158.

Lapidos, K. A., Kakkar, R., & McNally, E. M. (2004). The dystrophin glycoprotein complex: signaling strength and integrity for the sarcolemma. *Circ Res 94*, 1023–1031.

Li, D., Tapscoft, T., Gonzalez, O., Burch, P. E., Quinones, M. A., Zoghbi, W. A., et al. (1999). Desmin mutation responsible for idiopathic dilated cardiomyopathy. *Circulation 100*, 461–464.

Lockett, M. F. (1965). Dangerous effects of isoprenaline in myocardial failure. *Lancet 19*, 104–106.

Lohse, M. J., Engelhardt, S., & Eschenhagen, T. (2003). What is the role of β-adrenergic signaling in heart failure? *Circ Res 93*, 896–906.

Luscher, M. S., Thygesen, K., Ravkilde, J., & Heickendorff, L. (1997). Applicability of cardiac troponin T and I for early risk stratification in unstable coronary artery disease. TRIM Study Group. Thrombin inhibition in myocardial ischemia. *Circulation 96*, 2578–2585.

Macickova, T., Navarova, J., Urbancikova, M., & Horakova, K. (1999). Comparison of isoproterenol-induced changes in lysosomal enzyme activity in vivo and in vitro. *Gen Physiol Biophys 18*, 86–91.

Maeda, M., Biro, S., Kamogawa, Y., Hirakawa, T., Setoguchi, M., & Tei, C. (2003). Dystrophin upregulation in pressure-overloaded cardiac hypertrophy in rats. *Cell Motil Cytoskeleton 55*, 26–35.

Mellgren, R. L. (1980). Canine cardiac calcium-dependent proteases: resolution of two forms with different requirements for calcium. *FEBS Lett 109*, 129–133.

Matsumura, Y., Kusuoka, H., Inoue, M., Hori, M., & Kamada, T. (1993). Protective effect of the protease inhibitor leupeptin against myocardial stunning. *J Cardiovasc Pharmacol 22*, 135–142.

Michels, V. V., Moll, P. P., Miller, F. A., Tajik, A. J., Chu, J. S., Driscoll, D. J., et al. (1992). The frequency of familial dilated cardiomyopathy in a series of patients with idiopathic dilated cardiomyopathy. *N Engl J Med 326*, 77–82.

Nigro, V., Okazaki, Y., Belsito, A., Piluso, G., Matsuda, Y., Politano, L., et al. (1997). Identification of the Syrian hamster cardiomyopathy gene. *Hum Mol Genet 6*, 601–607.

Ohtsuki, I., Shiraishi, F., Suenaga, N., Miyata, T., & Tanokura, M. (1984). A 26K fragment of troponin T from rabbit skeletal muscle. *J Biochem (Tokyo) 95*, 1337–1342.

Olson, T. M., Michels, V. V., Thibodeau, S. N., Tai, Y. S., & Keating, M. T. (1998). Actin mutations in dilated cardiomyopathy, a heritable form of heart failure. *Science 280*, 750–752.

Ortiz-Lopez, R., Li, H., Su, J., Goytia, V., & Towbin, J. A. (1997). Evidence for a dystrophin missense mutation as a cause of X-linked dilated cardiomyopathy. *Circulation 95*, 2434–2440.

Packer, M., Coats, A. J., Fowler, M. B., Katus, H. A., Krum, H., Mohacsi, P., et al. (2001). Effect of carvedilol on survival in severe chronic heart failure. *N Engl J Med 344*, 1651–1658.

Politano, L., Nigro, V., Passamano, L., Petretta, V., Comi, L. I., Papparella, S., et al. (2001). Evaluation of cardiac and respiratory involvement in sarcoglycanopathies. *Neuromuscul Disord 11*, 178–185.

Poole-Wilson, P. A., Swedberg, K., Cleland, J. G., Di Lenarda, A., Hanrath, P., Komajda, M., et al. (2003). Comparison of carvedilol and metoprolol on clinical outcomes in patients with chronic heart failure in the Carvedilol Or Metoprolol European Trial (COMET): randomised controlled trial. *Lancet 362*, 7–13.

Ravichandran, L. V., Puvanakrishnan, R., & Joseph, K. T. (1991). Influence of isoproterenol-induced myocardial infarction on certain glycohydrolases and cathepsins in rats. *Biochem Med Metab Biol 45*, 6–15.

Saido, T. C., Shibata, M., Takenawa, T., Murofushi, H., & Suzuki, K. (1992). Positive regulation of μ-calpain action by polyphosphoinositides. *J Biol Chem 267*, 24585–24590.

Saido, T. C., Sorimachi, H., & Suzuki, K. (1994). Calpain: new perspectives in molecular diversity and physiological–pathological involvement. *FASEB J 8*, 814–822.

Sakamoto, A., Ono, K., Abe, M., Jasmin, G., Eki, T., Murakami, Y., et al. (1997). Both hypertrophic and dilated cardiomyopathies are caused by mutation of the same gene, δ-sarcoglycan, in hamster: an animal model of disrupted dystrophin-associated glycoprotein complex. *Proc Natl Acad Sci U S A 94*, 13873–13878.

Sandmann, S., Yu, M., & Unger, T. (2001). Transcriptional and translational regulation of calpain in the rat heart after myocardial infarction-effects of AT(1) and AT(2) receptor antagonists and ACE inhibitor. *Br J Pharmacol 132*, 767–777.

Sandmann, S., Prenzel, F., Shaw, L., Schauer, R., & Unger, T. (2002). Activity profile of calpains I and II in chronically infarcted rat myocardium-influence of the calpain inhibitor CAL 9961. *Br J Pharmacol 135*, 1951–1958.

Seidman, J. G., & Seidman, C. (2001). The genetic basis for cardiomyopathy: from mutation identification to mechanistic paradigms. *Cell 104*, 557–567.

Straub, V., Duclos, F., Venzke, D. P., Lee, J. C., Cutshall, S., Leveille, C. J., et al. (1998). Molecular pathogenesis of muscle degeneration in the δ-sarcoglycan-deficient hamster. *Am J Pathol 153*, 1623–1630.

Suzuki, K., Imajoh, S., Emori, Y., Kawasaki, H., Minami, Y., & Ohno, S. (1987). Calcium-activated neutral protease and its endogenous inhibitor. Activation at the cell membrane and biological function. *FEBS Lett 220*, 271–277.

Suzuki, K., Sorimachi, H., Yoshizawa, T., Kinbara, K., & Ishiura, S. (1995). Calpain: novel family members, activation, and physiologic function. *Biol Chem Hoppe Seyler 37*, 523–529.

Svensson, E. C., Marshall, D. J., Woodard, K., Lin, H., Jiang, F., Chu, L., et al. (1999). Efficient and stable transduction of cardiomyocytes after intramyocardial injection or intracoronary perfusion with recombinant adeno-associated virus vectors. *Circulation 99*, 201–205.

Takayasu, T., Toyo-oka, T., & Hosoda, S. (1990). Waste of ATP for tension development in myocardial acidosis: chemomechanical uncoupling at myofibrillar level. *J Mol Cell Cardiol 22*, 127–130.

Thomas, J. A., & Marks, B. H. (1978). Plasma norepinephrine in congestive heart failure. *Am J Cardiol 41*, 233–243.

Towbin, J. A., & Bowles, N. E. (2002). Molecular diagnosis of myocardial disease. *Expert Rev Mol Diagn 2*, 587–602.

Toyo-oka, T. (1982). Phosphorylation with cyclic adenosine 3′:5′ monophosphate-dependent protein kinase renders bovine cardiac troponin sensitive to the degradation by calcium-activated neutral protease. *Biochem Biophys Res Commun 107*, 44–50.

Toyo-oka, T., & Masaki, T. (1979). Calcium-activated neutral protease from bovine ventricular muscle: isolation and some of its properties. *J Mol Cell Cardiol 11*, 769–786.

Toyo-oka, T., & Nayler, W. G. (1996). Third generation calcium entry blockers. *Blood Press 5*, 206–208.

Toyo-oka, T., & Ross Jr., J. (1981). Ca^{2+} sensitivity change and troponin loss in cardiac natural actomyosin after coronary occlusion. *Am J Physiol 240*, H704–H708.

Toyo-oka, T., Shimizu, T., & Masaki, T. (1978). Inhibition of proteolytic activity of calcium activated neutral protease by leupeptin and antipain. *Biochem Biophys Res Commun 82*, 484–491.

Toyo-oka, T., Kamishiro, T., Masaki, M., & Masaki, T. (1982). Reduction of experimentally produced acute myocardial infarction size by a new synthetic inhibitor, NCO-700, against calcium-activated neutral protease. *Jpn Heart J 23*, 829–834.

Toyo-oka, T., Hara, K., Nakamura, N., Kitahara, M., & Masaki, T. (1985). Ca overload and the action of calcium sensitive proteases, phospholipases and prostaglandin E_2 in myocardial cell degradation. *Basic Res Cardiol 80*, 303–315.

Toyo-oka, T., Shin, W. S., Okai, Y., Dan, Y., Morita, M., Iizuka, M., et al. (1989). Collagen-stimulated human platelet aggregation is mediated by endogenous calcium-activated neutral protease. *Circ Res 64*, 407–410.

Toyo-oka, T., Morita, M., Shin, W. S., Okaimatsuo, Y., & Sugimoto, T. (1991). Contribution of calcium-activated neutral protease to the degradation process of ischemic heart. *Jpn Circ J 55*, 1124–1126.

Toyo-oka, T., Nagayama, K., Suzuki, J., & Sugimoto, T. (1992). Noninvasive assessment of cardiomyopathy development with simultaneous measurement of topical ^{1}H- and ^{31}P-magnetic resonance spectroscopy. *Circulation 86*, 295–301.

Toyo-oka, T., Kawada, T., Xi, H., Nakazawa, M., Masui, F., Hemmi, C., et al. (2002). Gene therapy prevents disruption of dystrophin-related proteins in a model of hereditary dilated cardiomyopathies in hamster. *Heart Lung Circ 11*, 174–181.

Toyo-oka, T., Kawada, T., Nakata, J., Xie, H., Urabe, M., Masui, F., et al. (2004). Translocation and cleavage of myocardial dystrophin as a common pathway to advanced heart failure: a scheme for the progression of cardiac dysfunction. *Proc Natl Acad Sci U S A 101*, 7381–7385.

Tsubata, S., Bowles, K. R., Vatta, M., Zintz, C., Titus, J., Muhonen, L., et al. (2000). Mutations in the human δ-sarcoglycan gene in familial and sporadic dilated cardiomyopathy. *J Clin Invest 106*, 655–662.

Vatta, M., Stetson, S. J., Perez-Verdia, A., Entman, M. L., Noon, G. P., Torre-Amione, G., et al. (2002). Molecular remodelling of dystrophin in patients with end-stage cardiomyopathies and reversal in patients on assistance-device therapy. *Lancet 359*, 936–941.

Wagner, J. A., Reynolds, T., Moran, M. L., Moss, R. B., Wine, J. J., Flotte, T. R., et al. (1998). Efficient and persistent gene transfer of AAV-CFTR in maxillary sinus. *Lancet 351*, 1702–1703.

Wheeler, M. T., Korcarz, C. E., Collins, K. A., Lapidos, K. A., Hack, A. A., Lyons, M. R., et al. (2004). Secondary coronary artery vasospasm promotes cardiomyopathy progression. *Am J Pathol 164*, 1063–1071.

Whitmer, J. T., Kumar, P., & Solaro, R. J. (1988). Calcium transport properties of cardiac sarcoplasmic reticulum from cardiomyopathic Syrian hamsters (BIO 53.58 and 14.6): evidence for a quantitative defect in dilated myopathic hearts not evident in hypertrophic hearts. *Circ Res 62*, 81–85.

Xi, H., Shin, W. S., Suzuki, J., Nakajima, T., Kawada, T., Uehara, Y., et al. (2000). Dystrophin disruption might be related to myocardial cell apoptosis caused by isoproterenol. *J Cardiovasc Pharmacol 36*(Suppl 2), S25–S29.

Xiao, X., Li, J., & Samulski, R. J. (1996). Efficient long-term gene transfer into muscle tissue of immunocompetent mice by adeno-associated virus vector. *J Virol 70*, 8098–8108.

Yoshida, K., Inui, M., Harada, K., Saido, T. C., Sorimachi, Y., Ishihara, T., et al. (1995). Reperfusion of rat heart after brief ischemia induces proteolysis of calspectin (nonerythroid spectrin or fodrin) by calpain. *Circ Res 77*, 603–610.

Yoshida, H., Takahashi, M., Koshimizu, M., Tanonaka, K., Oikawa, R., Toyo-oka, T., et al. (2003). Decrease in sarcoglycans and dystrophin in failing heart following acute myocardial infarction. *Cardiovasc Res 59*, 419–427.

British Journal of Pharmacology (2005) 146, 49–59
www.nature.com/bjp

Molecular and pharmacological characteristics of transient voltage-dependent K^+ currents in cultured human pulmonary arterial smooth muscle cells

[1]Haruko Iida, [1]Taisuke Jo, [1]Kuniaki Iwasawa, [1]Toshihiro Morita, [2]Hisako Hikiji, [2]Tsuyoshi Takato, [1]Teruhiko Toyo-oka, [1]Ryozo Nagai & *,[1,3]Toshiaki Nakajima

[1]Department of Cardiovascular & Respiratory Medicine, University of Tokyo, 7-3-1 Hongo, Bunkyo-ku, Tokyo 113-0033, Japan; [2]Department of Oral and Maxillofacial Surgery, University of Tokyo, 7-3-1 Hongo, Bunkyo-ku, Tokyo 113-0033, Japan and [3]Department of Ischemic Circulatory Physiology, University of Tokyo, 7-3-1 Hongo, Bunkyo-ku, Tokyo 113-0033, Japan

1 The A-type voltage-dependent K^+ current (I_A) has been identified in several types of smooth muscle cells including the pulmonary artery (PA), but little is known about the pharmacological and molecular characteristics of I_A in human pulmonary arterial smooth muscle cells (hPASMCs). We investigated I_A expressed in cultured PASMCs isolated from the human main pulmonary artery, using patch-clamp techniques, reverse transcriptase–polymerase chain reaction (RT–PCR), quantitative real-time RT–PCR and immunocytochemical studies.

2 With high EGTA and ATP in the pipette, the outward currents were dominated by a transient K^+ current (I_A), followed by a relatively small sustained outward current (I_K).

3 I_A was inhibited by 4-aminopyridine (4-AP) concentration-dependently, and could be separated pharmacologically into two components by tetraethylammonium (TEA) sensitivity. A component was sensitive to TEA, and the second component was insensitive to TEA.

4 I_A was inhibited by blood depressing substrate (BDS)-II, a specific blocker of $K_V3.4$ subunit, and phrixotoxin-II, a specific blocker of $K_V4.2$ and 4.3.

5 Flecainide inhibited I_A concentration-dependently, but it inhibited it preferentially in the presence of TEA (TEA-insensitive I_A).

6 Systematic screening of expression of K_V genes using RT–PCR showed the definite presence of transcripts of the I_A-encoding genes for $K_V3.4$, $K_V4.1$, $K_V4.2$ and $K_V4.3$ as well as the I_K-encoding genes for $K_V1.1$, $K_V1.5$ and $K_V2.1$. The real-time RT–PCR analysis showed that the relative abundance of the encoding genes of I_A α-subunit and K_V channel-interacting proteins (KChIPs) was $K_V4.2 > K_V3.4 > K_V4.3$ (long) $> K_V4.1$, and KChIP3 $\gg$ KChIP2, respectively.

7 The presence of $K_V3.4$, $K_V4.2$ and $K_V4.3$ proteins was also demonstrated by immunocytochemical studies, and confirmed by immunohistochemical staining using intact human PA sections.

8 These results suggest that I_A in cultured hPASMCs consists of two kinetically and pharmacologically distinct components, probably $K_V3.4$ and K_V4 channels.
British Journal of Pharmacology (2005) **146,** 49–59. doi:10.1038/sj.bjp.0706285;
published online 6 June 2005

Keywords: Human pulmonary arterial smooth muscle cells; voltage-dependent K^+ channel; $K_V3.4$; $K_V4.2$; $K_V4.3$; KChIPs; A-type voltage-dependent K^+ current; human pulmonary artery; RT–PCR; quantitative real-time RT–PCR

Abbreviations: 4-AP, 4-aminopyridine; BDS-II, blood depressing substance-II; CTX, charybdotoxin; $[Ca^{2+}]_i$, intracellular Ca^{2+} concentration; DTX, dendrotoxin; hPASMCs, human pulmonary arterial smooth muscle cells; I_A, transient outward current; I_{Ca}, voltage-dependent Ca^{2+} channels; KChIP, K_V channel-interacting protein; K_V, voltage-dependent K^+ channel; PA, pulmonary artery; PASMCs, pulmonary arterial smooth muscle cells; RT–PCR, reverse transcriptase–polymerase chain reaction; TEA, tetraethylammonium

Introduction

Voltage-dependent K^+ channels (K_V) are important in the regulation of membrane potential and the maintenance of vascular tone in vascular smooth muscle cells including pulmonary arterial smooth muscle cells (PASMCs) (Nelson & Quayle, 1995; Yuan, 1995; Turner & Kozlowski, 1997; Gurney *et al.*, 2003). Activation of K_V increases K^+ efflux, resulting in membrane hyperpolarization, which leads to closure of the voltage-dependent Ca^{2+} channels (I_{Ca}), reduced Ca^{2+} entry and subsequent vasodilation. Inhibition of K_V causes depolarization of the membrane to a threshold that opens I_{Ca}, increases Ca^{2+} entry, and causes vasoconstriction. Therefore, the normal function and expression of K_V are essential to maintain the vascular tone of PASMCs. Changes in K_V expression and function are linked to many patho-

*Author for correspondence at: Department of Ischemic Circulatory Physiology, University of Tokyo, 7-3-1 Hongo, Bunkyo-ku, Tokyo 113-0033, Japan; E-mail: masamasa@pb4.so-net.ne.jp

physiological conditions. Hypoxia and drugs such as fenfluramine affect the function and expression of K_V (Weir *et al.*, 1996; Patel *et al.*, 1997; Wang *et al.*, 1998; Hulme *et al.*, 1999; Perez-Garcia *et al.*, 2000; Yuan, 2001; Patel & Honore, 2001; Platoshyn *et al.*, 2001). In addition, dysfunction of K_V is known in the PASMCs obtained from patients with primary pulmonary hypertension (Yuan JX *et al.*, 1998).

K_V currents can be divided into two types in smooth muscle cells including PASMCs: delayed rectifier K^+ current (I_K) and transient outward current (I_A). The diversity of subunits underlying K_V allows the formation of channels with different properties (Stuhmer *et al.*, 1998; Coppock & Tamkun, 2001; Davies & Kozlowski, 2001). I_K shows delayed activation and slow inactivation, and is involved in modulating membrane potential and vascular tone in vessels such as the pulmonary artery (PA) (Osipenko *et al.*, 1997; Turner & Kozlowski, 1997; Archer *et al.*, 1998; Gurney *et al.*, 2003). On the other hand, I_A shows rapid activation and inactivation upon depolarization. I_A is not ubiquitous in smooth muscles, but affects membrane excitability, which has been identified in various PASMCs including human (Okabe *et al.*, 1987; Clapp & Gurney, 1991; James *et al.*, 1995; Yuan, 1995; Amberg *et al.*, 2002). Several K_V subunits have been cloned that can form I_A (Baldwin *et al.*, 1991; Pak *et al.*, 1991; Rudy *et al.*, 1991; Schroter *et al.*, 1991; Stuhmer *et al.*, 1998) including $K_V4.1$, $K_V4.2$ and $K_V4.3$ of Shal, $K_V3.3$ and $K_V3.4$ of Shaw and $K_V1.4$ of Shaker. Additionally, K_V1 may form rapidly inactivating K^+ channels when bound to accessory β-subunits (Rettig *et al.*, 1994; Heinemann *et al.*, 1996). By reverse transcriptase–polymerase chain reaction (RT–PCR), Western blotting and immunohistochemistry, both gene and protein expression for various K_V α-subunits have been identified in rat PASMCs (Archer *et al.*, 1998; Yuan XJ *et al.*, 1998; Davies & Kozlowski, 2001; Coppock & Tamkun, 2001; Yuan, 2001). RT–PCR has detected I_A-related genes ($K_V1.4$, $K_V4.1$, $K_V4.2$ and $K_V4.3$) in freshly isolated and primary cultured rat PASMCs (Yuan XJ *et al.*, 1998; Davies & Kozlowski, 2001; Platoshyn *et al.*, 2001; Yuan, 2001), but the molecular and pharmacological diversity of I_A-related K_V α-subunits and K_V channel-interacting protein (KChIP) (An *et al.*, 2000; Bahring *et al.*, 2001), an accessory subunit of K_V4 series, has not been investigated in human PASMCs (hPASMCs).

The present study investigated the molecular and pharmacological characteristics of I_A in cultured hPASMCs, using patch-clamp techniques, RT–PCR, quantitative real-time RT–PCR and immunocytochemical studies.

Methods

Cell preparation

Cultured cells isolated from normal human main pulmonary artery (hPASMCs) were purchased from Clonetics Corporation (San Diego, U.S.A.). The cells used for this study were obtained from six donors. The cells were cultured in 78.5 cm^2 flasks, in culture medium supplemented with 5% fetal calf serum, human epidermal growth factor (0.5 $\mu g\,ml^{-1}$), insulin (5 $mg\,ml^{-1}$), human fibroblast growth factor (1 $\mu g\,ml^{-1}$), gentamicin (50 $\mu g\,ml^{-1}$) and amphotericin B (0.05 $\mu g\,ml^{-1}$) (SmGM-2 Buffer-Kit, Clonetics) in an atmosphere of 5% CO_2 and 95% air at 37°C. At confluence, cells obtained from 78.5 cm^2 flasks were passaged using 0.25–0.5% trypsin in 0.02% EDTA. The medium was replaced twice weekly. Cells just at confluence of passages 3–8 were detached from the culture flasks with 0.25–0.5% trypsin in 0.02% EDTA, and used for later experiments. The cells were identified as smooth muscle cells, by staining α-actin, but not fibroblast growth factor, by immunostaining with biotin-conjugated antibody. All experiments were performed at 35–37°C.

Solutions and agents

The composition of control extracellular Tyrode solution was as follows (in mM): NaCl 136.5, KCl 5.4, $CaCl_2$ 1.8, $MgCl_2$ 0.53, glucose 5.5 and HEPES–NaOH buffer 5.5 (pH 7.4). The patch pipette contained (in mM): KCl 140, EGTA 10, $MgCl_2$ 2, Na_2ATP 3, guanosine-5′-triphosphate (GTP, sodium salt, Sigma) 0.1 and HEPES–KOH buffer 5 (pH 7.2). 4-Aminopyridine (4-AP), tetraethylammonium (TEA), charybdotoxin (CTX), dendrotoxin (DTX) and clofilium were purchased from Sigma (St Louis, MO, U.S.A.). Blood depressing substrate (BDS)-II and phrixotoxin-II were purchased from Alomone Ltd (Jerusalem, Israel). Flecainide was obtained from Eisai Company (Tokyo, Japan).

Recording technique and data analysis

Membrane currents were recorded with glass pipettes under whole-cell clamp conditions (Hamill *et al.*, 1981; Nakajima *et al.*, 1999), using a patch-clamp amplifier (EPC-7, List Electronics, Darmstadt, Germany). The heat-polished patch electrode had a tip resistance of 3–5 MΩ. The series resistance was compensated, and the raw data were subtracted by leakage currents. All data were acquired, stored and analyzed using a Power Macintosh 7100/80 with the PULSE+PULSEFIT software (HEKA Electronic) and Igor PRO (Wave Metrics, Lake Oswego, OR, U.S.A.) as described previously (Terasawa *et al.*, 2002).

The steady-state inactivation of I_A was estimated using the double-pulse protocol. Conditioning voltage pulses (500 ms duration) to various membrane potentials between −80 and +10 mV were applied from a holding potential of −80 mV. At 10 ms after the end of each conditioning pulse, a test pulse to +40 mV (400 ms duration) was applied to activate I_A. The ratio of I_A amplitude with and without conditioning pulses was plotted against each conditioning voltage. The steady-state activation curve was obtained from the conductance (G_K), determined by dividing the peak current amplitude at each membrane potential (V_m) by the driving force for K^+ ($V_m - E_K$), where E_K is the K^+-equilibrium potential. The time course of recovery from inactivation was measured by double-pulse protocols. The first (PI, 400 ms) and the second pulse (PII, 400 ms) with variable interpulse intervals were applied from −80 to +40 mV.

Data were expressed as mean ± s.e.m. Student's *t*-test was used for statistical analysis and $P<0.05$ was considered significant.

RNA extraction and RT–PCR

Total cellular RNA was extracted using Gene Elute™ Mammalian Total RNA Miniprep Kit (Sigma). For RT–PCR, cDNA (complementary DNA) was synthesized from 1 μg of total RNA with RT with random primers (Toyobo,

Osaka) (Oonuma *et al.*, 2002). The reaction mixture was then subjected to PCR amplification with specific forward and reverse oligonucleotide primers for 35 cycles consisting of heat denaturation, annealing and extension. PCR products were size fractionated on 2% agarose gels, and visualized under UV light. Primers were chosen on the basis of the sequences of human K_V1.1-6, K_V2.1-2, K_V3.1-4 and K_V4.1-3 as shown in Table 1. Total RNA from the human fetal brain (Toyobo, Osaka) was used as a positive control.

Real-time quantitative RT–PCR was performed with the use of real-time Taq-Man technology and a sequence detector (ABI PRISM® 7000, Applied Biosystems, Foster City, CA, U.S.A.). Gene-specific primers and Taq-Man probes were used to analyze transcript abundance. The 18S ribosomal RNA level was analyzed as an internal control and used to normalize the values for transcript abundance of K_V α-subunit family genes and KChIPs family genes. We performed six independent experiments.

Immunocytochemistry

Immunocytochemical analysis for the presence of K_V used polyclonal antibodies against K_V3.4. (Alomone Labs, Jerusalem), K_V4.2 (N-15) and K_V4.3 (C-17) (Santa Cruz Biotechnology Inc., CA, U.S.A.). HPASMCs were cultured on Lab-Tek Chamber Slide Glass (Nalge Nunc International, Naperville), fixed with 2% paraformaldehyde for 45 min, rinsed in phosphate-buffered saline (PBS), then blocked in 0.2% Triton X-100 (Sigma), 1% H_2O_2 in PBS. The cells were rinsed in PBS, and incubated in Block Ace (Dainippon Seiyaku, Osaka, Japan) for 30 min at 37°C. The hPASMCs were then incubated with the primary antibodies overnight at 4°C. For control sections, cells were incubated with Block Ace without primary antibody. Cells were then rinsed in PBS, incubated in biotinylated anti-rabbit IgG or anti-goat IgG (Vector Lab. Inc.) for 30 min at room temperature, rinsed in PBS, incubated in VECTASTAIN ABC kit (Vector Lab. Inc., Burlingame) for 20 min at room temperature, and rinsed in PBS. 3,3′-Diaminobenzidine, tetrahydrochloride (DAB, Dojin, Kumamoto) with 0.06% H_2O_2 in PBS was used to form a colored reaction product. Cells were dehydrated, and cover slides were placed on the slides, and viewed using an Olympus BH-2 microscope (Tokyo).

Immunohistochemistry

Immunohistochemical analysis for the presence of voltage-gated K^+ channels used polyclonal antibodies against K_V3.4, K_V4.2 and K_V4.3. Paraffin-embedded human pulmonary artery sections on glass slides (Human Adult Normal Arteriae Pulmonalis Tissue Slide for main PA and Human Adult Normal Urinary & Respiratory System Multi-Tissue Slide for small PA) were purchased from Biochain Institute Inc. (Hayward, CA, U.S.A.). The glass slides were deparaffinized and rehydrated, and the following process was the same as described for immnocytochemistry.

Results

4-AP-sensitive I_A in cultured hPASMCs

Figure 1a shows typical original current traces recorded with 3 mM ATP and 10 mM EGTA. The cells were held at −70 mV,

Table 1 PCR primers used for amplification of voltage-dependent K^+ channel genes

	Size (bp)		*Sequence ('5-'3)*
Kv1.1	352	Sense	ACC GAG ATA GCT GAG CAG GA
		Antisense	CGA TCT TGC CTC CAA TTG TC
Kv1.2	538	Sense	AGA CCA CGA GTG CTG TGA GA
		Antisense	GGA ATA GGT GTG GAA GGT CA
Kv1.3	457	Sense	TTC GGT GTC CCT ACC CTG TA
		Antisense	GGA AAC ATG GGT TGC TAT GG
Kv1.4	506	Sense	GCT TCC CTC ATT GCT CTG AC
		Antisense	AAA CTT CAA CAG GGC CTC CT
Kv1.5	685	Sense	GTG TAA CGT CAA GGC CAA GAG CAA C
		Antisense	AGA CAG AGG CTT GGA GAC ACA GGA A
Kv1.6	590	Sense	CAA TGG TGG TGT GAG TCG AG
		Antisense	AAT CGT CAT CGT CAG CCT CT
Kv2.1	641	Sense	GTC TCT GGG CTT CAC TTT GC
		Antisense	TGT CTT CCA ACT GCT GAA CG
Kv2.2	245	Sense	CTG GAA GTG TGC GAC GAC TA
		Antisense	TCT CGC CTC AGT TCT TCG TT
Kv3.1	198	Sense	CTG GTC TCC ATC ACC ACC TT
		Antisense	GAA GAT GAC ACG CAT GAG GA
Kv3.2	255	Sense	GTA CCC CCA AAC ATG GTC AG
		Antisense	TTG CCC AGA CAT GTG TCA CT
Kv3.3	308	Sense	CCC AGA CAA GGT GGA GTT TC
		Antisense	CAA TGC GCT CAG CGT AGT AA
Kv3.4	346	Sense	AGA GAC AGA GCC CAT CCT GA
		Antisense	CAG GGC CAG GAA GAT GAT AA
Kv4.1	410	Sense	GGC TCT TTG TGT CAG GAA CC
		Antisense	TGC TGA TAA TGG CAG CTA CG
Kv4.2	301	Sense	GCC TTC TTC TGC TTG GAC AC
		Antisense	GCA AGA AGC CCA ATT CTG AG
Kv4.3	359	Sense	ATC TTC ACC GGG GAG TAC CT
		Antisense	GGG ATG CTT GTG AAC TTG CT

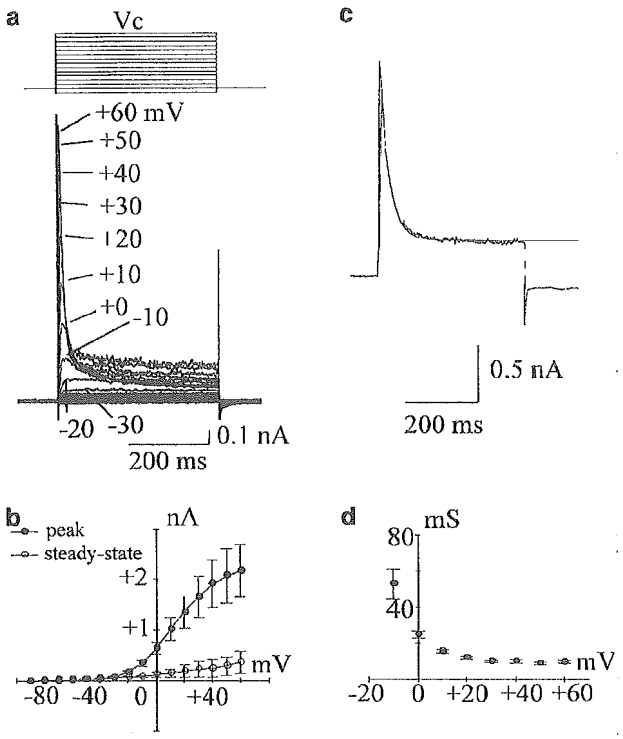

Figure 1 (a) Membrane currents measured with patch pipettes containing 3 mM ATP and 10 mM EGTA. (b) The current–voltage (I–V) relationships measured at the peak (close circles) and steady state (open circles). The data were obtained from six different cells. (c, d) Time courses of inactivation of I_A. The time courses of inactivation of I_A were fitted approximately by single exponential function (c). In (d), the mean±s.e.m. values obtained from three different cells are presented.

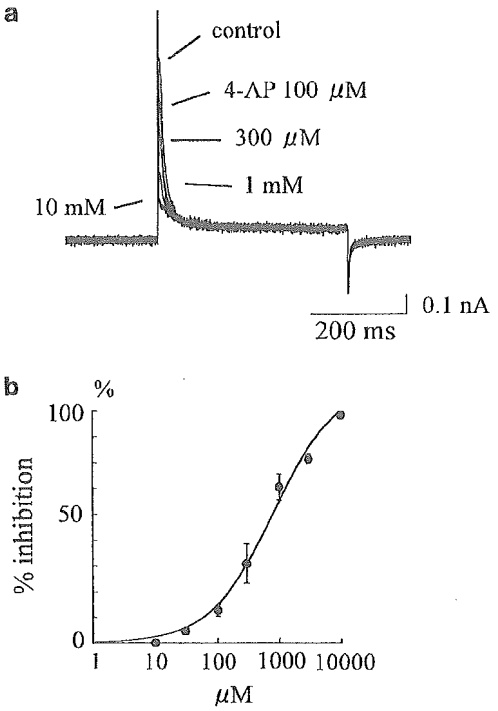

Figure 2 Effects of 4-AP on I_A. (a) Effects of various concentrations of 4-AP. The currents traces are shown in control and in the presence of various concentrations of 4-AP. The cells were held at −80 mV, and command voltage pulses to +40 mV were applied. (b) Concentration-dependent inhibitory effects of 4-AP. Data are shown as mean±s.e.m. (n=3–5), and fit by a Hill equation: % inhibition = $100/\{1+([IC_{50}]/[4\text{-AP}])^n\}$, where n represents Hill coefficient, and IC_{50} is 50% inhibitory concentration for 4-AP. The data were best fit with an IC_{50} value of 794 μM and n of 0.8.

and the command voltage pulses to various membrane potentials were applied. During depolarizing pulses, the outward currents with a threshold potential of approximately −40 mV were activated. The currents were rapidly activated, and then rapidly declined to a relatively low steady-state level. Figure 1b shows the current–voltage (I–V) relationships of the outward currents measured at the peak and the steady state. The transient outward current (I_A) and the steady-state outward current (I_K) both increased with depolarization. Figure 1c and d illustrate the time courses of inactivation of I_A. We calculated τ by fitting the I_A decay with a single exponential, and typical data are shown in Figure 1c. The mean±s.e.m. values (n=3) are plotted in Figure 1d against each command potential.

Figure 2 shows the effects of 4-AP on membrane currents. 4-AP inhibited I_A concentration-dependently (Figure 2a), and the half-maximal inhibitory concentration (IC_{50}) was 794 μM (Figure 2b, n=3–5).

RT–PCR and quantitative real-time RT–PCR analysis of K_V α-subunit and KChIP mRNA expression

The above results show the existence of 4-AP-sensitive I_A in cultured hPASMCs. Therefore, we investigated the systematic screening of the expression of K_V genes using RT–PCR (Figure 3). Definite expression of the transcripts of I_A α-subunit-encoding genes (K_V3.4, K_V4.1, K_V4.2 and K_V4.3) as well as I_K-encoding genes (K_V1.1, K_V1.5 and K_V2.1) was observed. However, no definite expression of K_V1.4 and K_V3.3 mRNA was observed. The identity of all K_V homologs seen by RT–PCR was performed by sequencing the relevant band excised from gel to confirm the identity of the product obtained. The quantitative expression of I_A α-subunit-encoding genes (K_V1.4, K_V3.3, K_V3.4, K_V4.1, K_V4.2 and K_V4.3) was investigated by real-time RT–PCR. Transcript levels were normalized to 18S ribosomal housekeeping gene. K_V4.3 appears to be alternatively spliced (Ohya *et al.*, 1997), and the expression of K_V4.3 (long) and K_V4.3 (short) was investigated. As shown in Figure 4a, the relative abundance of the encoding genes of I_A α-subunit was K_V4.2>K_V3.4>K_V4.3 (long)>K_V4.1 with a ratio of 1.00:0.55:0.20:0.09. However, no definite expression of K_V3.3 and K_V4.3 (short) was detected. Thus, it is likely that I_A consists of K_V3.4 and K_V4 currents.

The expression of KChIP, an accessory subunit of K_V4 series, was also investigated by real-time RT–PCR analysis (Figure 4b). KChIP was mainly composed of KChIP3. Neither KChIP1 nor KChIP4 was detected significantly.

Immunocytochemical and immunohistochemical detection of K_V3.4. and K_V4 proteins

Figure 5 shows typical immunocytochemical images obtained from cultured hPASMCs containing I_A in electro-

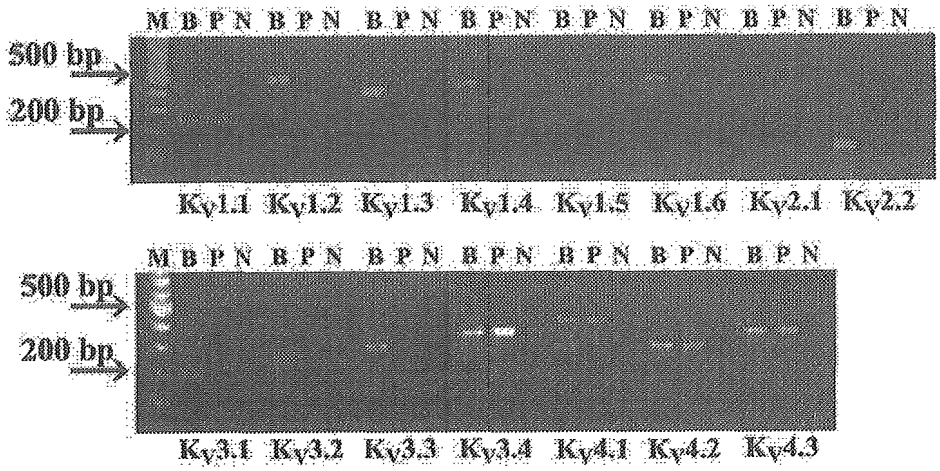

Figure 3 Analysis of K_V mRNA by RT–PCR. Ethidiumbromide-stained gel of RT–PCR products for K_V1.1-6, K_V2.1-2, K_V3.1-4 and K_V4.1-3 mRNA. M, marker; N, negative control; B, human brain; P, cultured hPASMCs.

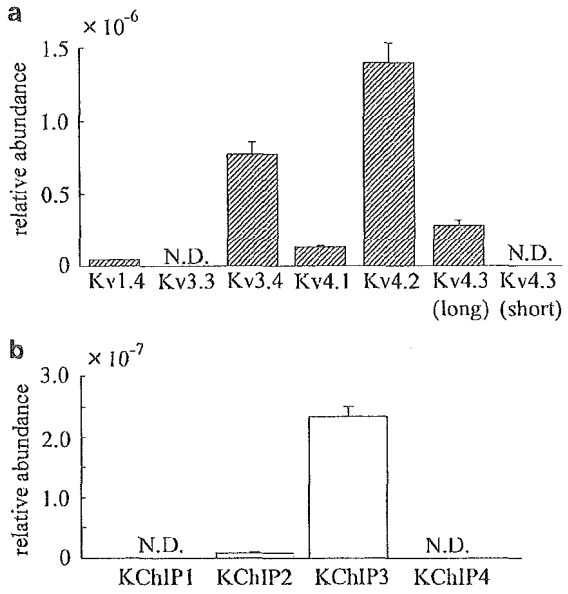

Figure 4 Expression of I_A α-subunit-encoding mRNA (a) and KChIPs mRNA (b) in cultured hPASMCs. The expression levels of I_A α-subunit-encoding genes (K_V1.4, K_V3.3, K_V3.4, K_V4.1, K_V4.2 and K_V4.3 (long and short)) and KChIPs (KChIP1, KChIP2, KChIP3 and KChIP4) genes were normalized to those of the 18S ribosomal RNA levels. Data are means±s.e.m. from six independent samples.

physiological studies. The immunocytochemical studies showed that the cells were immunostained positively with anti-K_V3.4 (Figure 5a). Expression of K_V4.2 and K_V4.3 (Figure 5a) protein was also detected in cultured hPASMCs. Similar results were obtained from three different experiments in each case.

Immunohistochemical studies using hPA sections revealed K_V3.4, K_V4.2 and K_V4.3-like immunoreactivity in intact hPASMCs, as shown in Figures 5b (main PA) and Figure 5c (small PA).

Effects of various K^+ channel blockers on I_A

To investigate the pharmacological characteristics of I_A, the effects of various K^+ channel blockers on I_A were examined. Figure 6A shows the effects of low concentration of TEA (1 mM), which preferentially inhibits K_V3.4 compared with K_V4 currents. The cells were held at −80 mV, and command voltage steps to +40 mV were applied. TEA (1 mM) markedly reduced the amplitude of I_A, but higher concentrations of TEA (10 mM) only caused a slight further reduction. The *I–V* relationships measured at the peak and the steady state were plotted in control ($n=6$, Figure 6B, open circle and square) and in the presence of TEA (10 mM, closed circle and square). I_A consisted of a TEA-sensitive component (71.8±6.4% of control I_A in a cell), and a TEA-insensitive component (28.2±6.4%, $n=12$) (Figure 7). Approximately 10% of the cells tested had only TEA-sensitive I_A.

Figures 6C, D and 7 show the effects of BDS-II, a specific blocker of K_V3.4 (Diochot *et al.*, 1998), and phrixotoxin-II, a specific blocker of K_V4.2 and K_V4.3 (Chagot *et al.*, 2004). BDS-II (3 μM) markedly reduced I_A by 67.0±4.7% ($n=3$, Figures 6Ca and 7). It failed to inhibit I_A recorded in the presence of TEA (10 mM, $n=3$, Figure 6Cb) significantly, suggesting that BDS-II selectively inhibited TEA-sensitive I_A in cultured hPASMCs. On the other hand, phyrixotoxin-II (1 μM) reduced it by 36.5±2.0% ($n=3$, Figure 6Da and 7), but it failed to inhibit I_A recorded in a cell containing only TEA-sensitive I_A ($n=3$, Figure 6Db). DTX (100 nM) and CTX (100 nM) inhibited I_A by only 3.0±0.6% ($n=4$) and 1.8±0.6% ($n=4$), respectively (Figure 7). Clofilium (10–50 μM, Figure 7) inhibited I_A by only 2.6±1.1% at 10 μM, and 6.3±1.4% at 50 μM ($n=4$).

The effects of flecainide on I_A are shown in Figure 8. The current traces are shown for the control (Figure 8a) and in the presence of flecainide (10–100 μM, Figure 8a). The *I–V* relationships (Figure 8b, $n=6$) measured at the peak and the steady state are indicated in control and in the presence of flecainide. Flecainde (100 μM) decreased the amplitude of I_A at all command voltages, and inhibited it concentration-dependently. The IC_{50} value of flecainide on control I_A was 113 μM

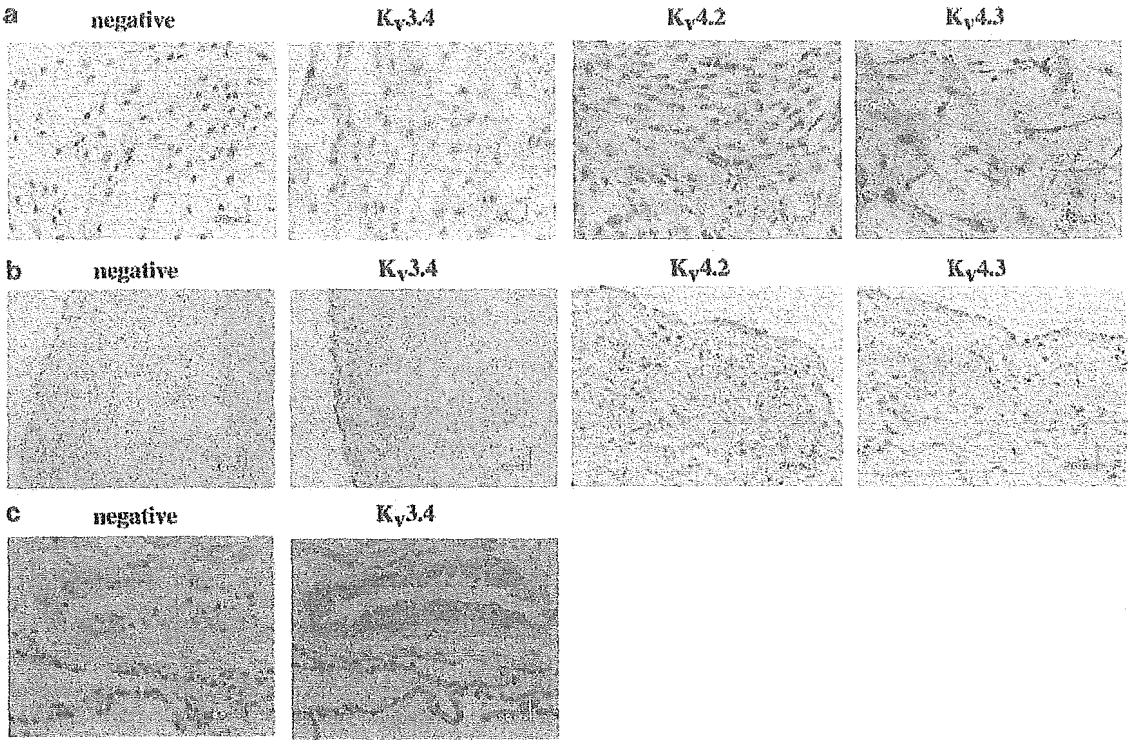

Figure 5 Immunocytochemical and immunohitochemical detection of $K_V3.4$, $K_V4.2$ and $K_V4.3$ protein in cultured hPASMCs (a) and intact human main PA (b) and small PA (c). (a) Expression of $K_V3.4$, $K_V4.2$ and $K_V4.3$ protein in cultured hPASMCs. In the negative control, cells were counterstained with hematoxylin in the absence of anti-$K_V3.4$. (b, c) Immunohistochemical detection of $K_V3.4$, $K_V4.2$ and $K_V4.3$ protein in intact human main PA (b) and small PA (c). Negative controls are shown in each case.

($n=5$). In addition, to compare the effects of flecainide on both TEA-insensitive and TEA-sensitive I_A separately, the effects of flecainide on each component of I_A were examined in a cell containing only TEA-sensitive I_A, and a cell bathed with TEA (10 mM). Flecainide inhibited it with an IC_{50} value of 30 μM in the presence of TEA (10 mM, Figure 8c, $n=4$, closed circles) and with an IC_{50} value of 160 μM in a cell containing only TEA-sensitive I_A (Figure 8c, $n=3$, closed squares).

Kinetics and voltage dependence of two different types of I_A

To clarify the characteristics of the two different types of I_A, the voltage dependence of inactivation of I_A was determined by two-step voltage pulses. Figure 9Aa and Ab show the data from a cell containing only TEA-sensitive I_A, and a cell bathed with TEA (10 mM). The peak amplitude of I_A at each test pulse was normalized to the maximal amplitude of I_A, and the normalized I_A was plotted against the conditioning voltages. The normalized values were fitted to Boltzmann equation using the least-squares methods:

$$I/I_{max} = 1/(1 + \exp[(V_m - V_h)/k])$$

where I gives the current amplitude and I_{max} is its maximum, V_m is the potential of the prepulse, V_h is the half-maximal inactivation potential, and k is the slope factor. The TEA-sensitive I_A showed a mean voltage at half inactivation of -23.2 mV, and k of 6.8 ($n=6$, Figure 9Ba), whereas the TEA-insensitive I_A showed values of -54.5 mV, and 7.3 ($n=4$, Figure 9Bb), respectively. The steady-state activation curves were obtained from the conductance as described in Methods, and also fitted to Boltzmann equation (Figure 9B):

$$G_K/G_{K.Max} = 1/(1 + \exp[-(V_m - V_h)/k])$$

where $G_{K.Max}$ is the maximal chord conductance, G_K is the chord conductance calculated at the membrane potential (V_m), V_h is the potential at which the conductance is one-half maximally activated and k is the slope factor. The TEA-sensitive I_A showed a mean voltage at half activation of -1.6 mV, and a slope factor of 6.9 ($n=5$, Figure 9Ba), whereas the TEA-insensitive I_A showed values of -2.4 mV and 17.8 ($n=6$, Figure 9Bb), respectively.

The time course of recovery of I_A from inactivation was investigated by the double-pulse protocol (Figure 9C). Figures 9Ca and Cb show the typical data recordings obtained from a cell containing only TEA-sensitive I_A, and a cell bathed with TEA (10 mM). The reactivation time course could be approximately fitted to a single exponential function (Figure 9D). The reactivation time constant was 1521.6 ± 101.4 ms ($n=5$) for the TEA-sensitive I_A, and 238 ± 30 ms ($n=3$) for the TEA-insensitive I_A.

Discussion

The present study showed that I_A in cultured hPASMCs includes two different types of I_A based on the pharmacological and electrophysiological characteristics. Systematic

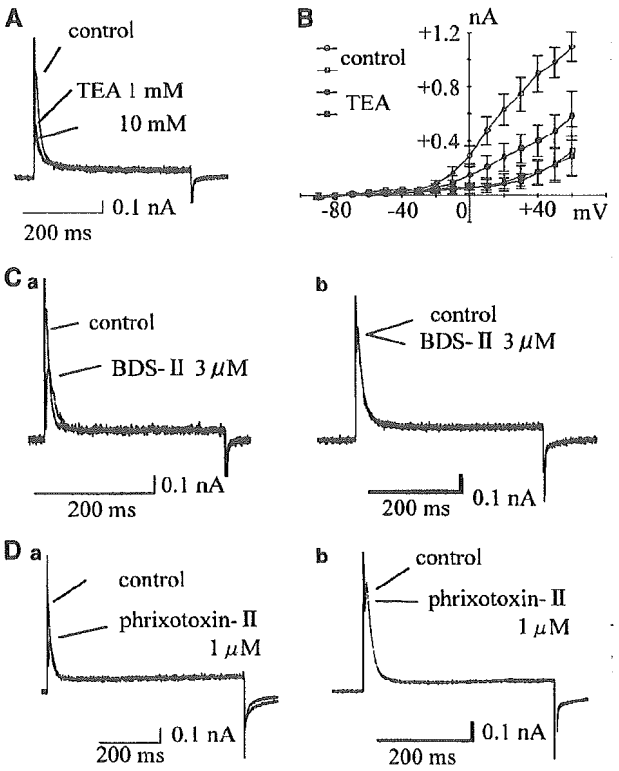

Figure 6 Effects of various K^+ channel blockers on I_A. (A) Effects of TEA (1–10 mM) on I_A. The cells were held at −80 mV, and command voltage pulses to +40 mV were applied at 0.2 Hz. (B) The *I–V* relationships measured at the peak (open and close circles), and the steady state (open and close squares) in control and in the presence of TEA (10 mM). The data are shown as mean±s.e.m. values ($n=6$). (C) Effects of BDS-II on I_A recorded in a control cell (a) and in a cell treated with TEA (10 mM, b). (D) Effects of phrixotoxin-II on I_A recorded in a control cell (a) and in a cell containing only TEA-sensitive I_A (b). Each datum is representative of three different cells.

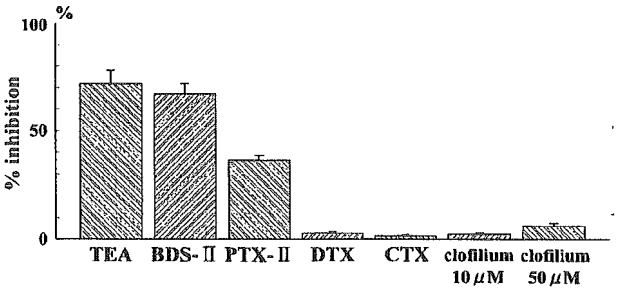

Figure 7 The percent inhibition of various K^+ channel blockers on I_A in cultured human PASMCs. TEA (10 mM, $n=12$), BDS-II (3 μM, $n=3$), phrixotoxin-II (PTX-II, 1 μM, $n=3$), dendrotoxin (DTX, 100 nM, $n=4$), charybdotoxin (CTX, 100 nM, $n=4$) and clofilium (10–50 μM, $n=4$). The cells were held at −80 mV, and command voltage pulses to +40 mV were applied at 0.2 Hz.

screening of the expression of I_A-coding genes using RT–PCR detected the transcripts of the genes encoding for $K_V3.4$, $K_V4.1$, $K_V4.2$ and $K_V4.3$, but not $K_V1.4$ or $K_V3.3$. The detailed quantitative RT–PCR analysis confirmed that the relative

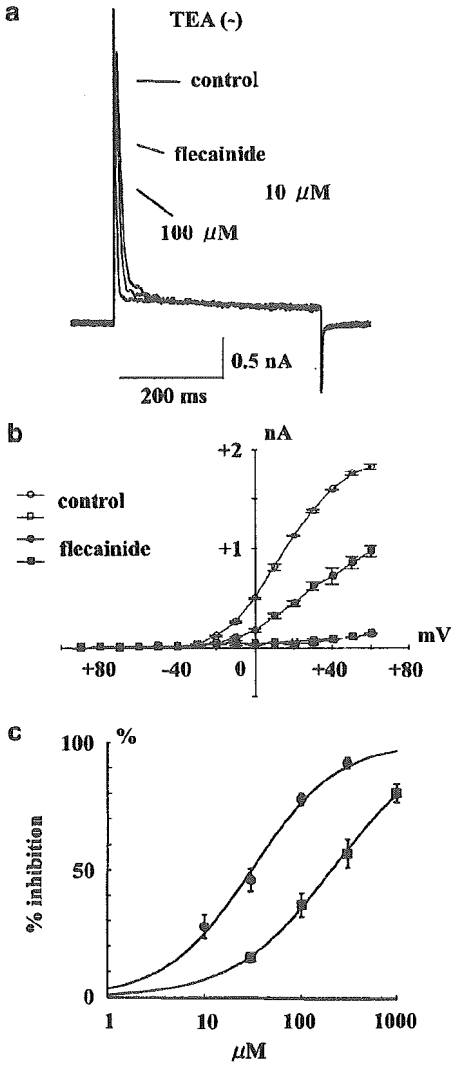

Figure 8 Effects of flecainide on I_A. (a) Effects of flecainide on I_A. The typical current traces are shown in control and after the application of flecainide (10–100 μM). The cells were held at −80 mV, and command voltage pulses to +40 mV were applied. (b) The current–voltage relationships measured at the peak and steady state in control (open circles and squares) and after the application of flecainde (100 μM, closed circles and squares). The data are shown as mean±s.e.m. values ($n=6$). (c) Concentration-dependent inhibitory effects of flecainide on I_A recorded in a cell containing only TEA-sensitive I_A (closed squares) and a cell bathed with TEA (10 mM, closed circles). Data are shown as mean±s.e.m. ($n=3$), and fitted by a Hill equation: % inhibition $= 100/\{1+(IC_{50}/[\text{flecainide}])^n\}$, where n represents Hill coefficient, and IC_{50} is 50% inhibitory concentration for flecainide. The data were best fit with an IC_{50} value of 160 μM in a cell containing only TEA-sensitive I_A, and an IC_{50} value of 30 μM in a cell bathed with TEA (10 mM).

abundance of I_A-encoding α-subunit expression was $K_V4.2 > K_V3.4 > K_V4.3$ (long), and KChIP, an accessory subunit of K_V4 series, was mainly composed of KChIP3. The electrophysiological, pharmacological and molecular analyses suggest that I_A in cultured hPASMCs consists of $K_V3.4$ and K_V4 plus KChIP3, which were also confirmed by immunocytochemical studies in cultured hPASMCs and intact PA sections.

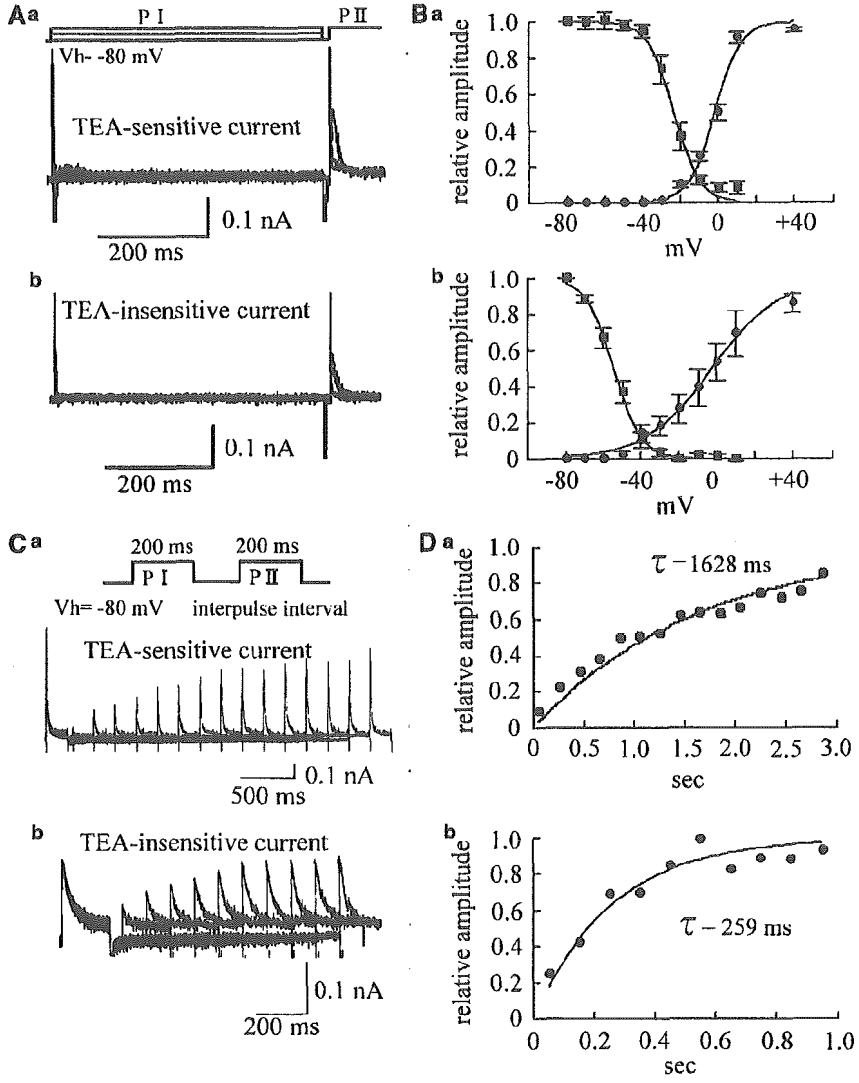

Figure 9 Two components of I_A. (A, B) Steady-state inactivation and activation curves for I_A. Using the double pulse protocol, the steady-state inactivation parameter for I_A was obtained from a cell (Aa), in which only TEA-sensitive current was present, and a cell bathed with TEA (Ab, 10 mM). The typical data were fitted by Boltzmann equation as shown in (B). The steady-state activation curves were also indicated in (B). The mean ± s.e.m. values obtained from four to six different cells. (C, D) Recovery from inactivation of I_A. The data in (C) were obtained from a cell (Ca), where only TEA-sensitive current was present and a cell (Cb) bathed with TEA (10 mM). The fitted data are shown in (D). Each datum is representative of three to five different experiments.

K_V is involved in membrane excitability, and regulates $[Ca^{2+}]_i$ and vascular tone (Nelson & Quayle, 1995). 4-AP, a K_V channel blocker, caused depolarization of the membrane and increased $[Ca^{2+}]_i$ in cultured hPASMCs (data not shown) as found in several types of PASMCs including rat (Yuan, 1995; Weir *et al.*, 1996; Archer *et al.*, 1998). Molecular and electrophysiological studies have shown that I_K-encoding genes such as $K_V2.1$, which are oxygen-sensitive K_V, are involved in hypoxic vasoconstriction of rat PASMCs (Osipenko *et al.*, 1997; Turner & Kozlowski, 1997; Archer *et al.*, 1998; Patel & Honore, 2001; Gurney *et al.*, 2003). Our RT–PCR analysis also detected the I_K-encoding genes ($K_V1.5$ and $K_V2.1$) in cultured hPASMCs. However, in physiological studies, depolarizing pulses elicited I_A, followed by relatively small steady-state K^+ currents (I_K), as reported previously in cultured hPASMCs (James *et al.*, 1995). Therefore, the density of I_K appears to decrease during repetitive subculture as described in rat PASMCs (Yuan *et al.*, 1993). However, the small I_K facilitated the detailed discrimination and investigation of I_A in the present study.

The present study demonstrated the presence of two different types of I_A. 4-AP inhibited I_A with an IC_{50} value of 794 μM, and I_A could be divided into two different components by the sensitivity to TEA. One component was sensitive to low concentrations of TEA. These pharmacological properties were similar to the cloned $K_V3.4$ channel (Rudy *et al.*, 1991; Schroter *et al.*, 1991). Additionally BDS-II, a specific blocker of $K_V3.4$ (Diochot *et al.*, 1998), inhibited I_A, which also supports the existence of $K_V3.4$ channel. The other component of I_A was resistant to these agents, and inhibited by phrixotoxin-II, a selective blocker of $K_V4.2$ and $K_V4.3$ (Chagot *et al.*, 2004), suggesting that this component consists of K_V4